Resource Allocation for Multicarrier Device-to-Device Video Transmission: Symbol Error Rate Analysis and Algorithm Design

Peizhi Wu, *Student Member, IEEE*, Pamela C. Cosman, *Fellow, IEEE*, and Laurence B. Milstein, *Fellow, IEEE*

***Abstract*— In resource allocation for a device-to-device (D2D) video transmission system, the performance improvement by applying the exact symbol error rate (SER) is compared with the conventional signal-to-interference-plus-noise-ratio-based SER evaluation method that uses a Gaussian approximation (GA) for the aggregated interference. An analytical SER expression for a D2D system using multicarrier bandlimited QAM is derived and then used in the resource allocation algorithm. We consider centralized resource allocation for the D2D system, given knowledge of the channel state information and the rate distortion information of the video streams, and propose an iterative algorithm for subcarrier assignment and power allocation. Bit-level simulations for different numbers of D2D pairs demonstrate a considerable improvement on user capacity and video peak signal-to-noise ratio by incorporating the proposed SER expression compared with the GA. By invoking the conditions under which the central limit theorem holds, and comparing these conditions with the number of interferers and the power ratio of the dominant interferer in the simulated D2D system, we also study why the GA for the interference degrades performance.**

***Index Terms*— Device-to-device communication, multimedia communication, resource allocation, cochannel interference.**

I. Introduction

DEVICE-TO-DEVICE communication [1] is a paradigm that allows multiple transmitter-receiver pairs to share the same spectrum , thereby improving the spectral efficiency and offloading traffic from the base station. Interference is a key consideration in the design of a D2D communication system, since a D2D user operating on shared spectrum receives not only the desired signal but also signals from other D2D users. At present, Orthogonal Frequency Division Multiplexing (OFDM) [2] is a widely adopted waveform due to its simple implementation and robustness against multipath. However, the application scenarios predicted for D2D communications present transmission delays between multiple D2D pairs [3], making the strict synchronization to maintain orthogonality between subcarriers infeasible. Also, the intercarrier interference (ICI) due to the high out-of-band (OOB) emission of OFDM [4] poses a challenge. Therefore, OFDM is not the most promising waveform for D2D communications. In this context, Filter Bank Multicarrier (FBMC) based waveforms, such as Filtered Multi-Tone (FMT) [5], are currently being evaluated as candidates for the waveforms of D2D communications.

Signals from other D2D pairs on shared spectrum produce cochannel interference (CCI) at the D2D receiver. A well-known approach to treating CCI is to approximate the aggregated interference as a Gaussian random variable, based upon a Gaussian approximation (GA) of the interference in the test statistic. However, the GA heavily relies on the conditions that validate the central limit theorem, which may not be suitable for D2D systems. First, the spectrum of D2D systems is directly shared by users without the use of spread spectrum, so the number of interfering users can be small [6]. Also, one or a few of the interferers may have significantly larger power than other interferers at a D2D receiver.

To circumvent the inaccuracy of the GA, an analytical expression of the exact symbol error rate (SER) of digital systems under CCI is of great interest. Early endeavors to calculate the probability of error in a bandlimited digital system with interference were devoted to phase-shift keying (PSK), such as binary phase-shift keying (BPSK) [7]–[9] and quadrature phase-shift keying (QPSK) [10], [11]. Current multimedia applications often use quadrature amplitude modulation (QAM) for rate-adaptive transmission [12], due to its practicality and bandwidth efficiency. A vast literature has been dedicated to the performance analysis of QAM, such as [13], [14], but few papers were related to the performance analysis of bandlimited QAM corrupted by CCI. Unlike PSK, the symbols of high-order QAM, such as 16-QAM or 64-QAM, have multiple power levels. Also, the in-phase and quadrature components of a QAM CCI signal are correlated if a random phase shift is introduced, so it is necessary to jointly consider the detection in the in-phase and quadrature paths. Therefore, the treatments for PSK modulated CCI in [7]–[11] are not applicable to QAM modulated CCI. For bandlimited QAM under CCI, [15] proposed a simple upper bound to the probability of error based on the Chernoff bound, but the bound was not tight. In [16], the authors presented a saddlepoint integration method to numerically evaluate the

Manuscript received April 20, 2016; revised September 27, 2016; accepted October 19, 2016. Date of publication October 31, 2016; date of current version October 16, 2017. This research was supported in part by the Army Research Office under Grant W911NF-14-1-0340. This paper was presented at the IEEE GLOBECOM, Washington, DC, December 2016. The associate editor coordinating the review of this paper and approving it for publication was M. Uysal.

P. Wu was with the Department of Electrical and Computer Engineering, University of California at San Diego, La Jolla, CA 92093 USA. He is now with Qualcomm, San Diego, CA 92121 USA (e-mail: zephywu@gmail.com).

P. C. Cosman and L. B. Milstein are with the Department of Electrical and Computer Engineering, University of California at San Diego, La Jolla, CA 92093 USA (e-mail: pcosman@ucsd.edu; milstein@ece.ucsd.edu).

Color versions of one or more of the figures in this paper are available online at http://ieeexplore.ieee.org.

Digital Object Identifier 10.1109/TCOMM.2016.2623313

error probability of a bandlimited QAM system with interference. The authors of [17] derived a bit error rate (BER) expression for QAM systems with rectangular pulses corrupted by asynchronous CCI in Nakagami-m fading channels. However, the BER expression was given in an integral form, which limited its usefulness.

Centralized resource allocation for D2D systems was investigated in [18]–[21]. These papers aimed to maximize the weighted sum rate based on the capacity of the Gaussian channel, by assuming that the GA was valid for the interference. In addition, these works divided the spectrum into frequency-flat subcarriers and restricted every D2D user's access to the spectrum of a single subcarrier. Nevertheless, to fully exploit frequency diversity, D2D users can be assigned to multiple subcarriers, and the resultant optimization problem with a total power constraint resembles the discrete dynamic spectrum management (DSM) problem in [22] and [23]. For the multicarrier, multiuser setting, the discrete DSM problem was shown to be non-convex and thereby to be NP-hard [23].

For video delivery with delay constraints, forward error correction (FEC)-based transmission with no retransmission is usually used [24], which demands a low packet loss rate [25] or a low SER [26]. In [26], an iterative resource allocation algorithm for video transmission on cellular uplinks was proposed, where every subcarrier was assigned to a single user. However, for D2D systems, a subcarrier can be assigned to multiple users to improve spectral efficiency. Literature on resource allocation for D2D video delivery included optimization for energy efficiency subject to a QoS constraint [27], and for a utility function that was jointly determined by the throughput and transmission power [28]. Optimization for overall video quality of D2D transmission does not appear to have been addressed.

This paper is organized as follows. Section II describes the system model. Section III derives an analytical expression for the SER of bandlimited QAM under CCI. In Section IV, the optimization problem for resource allocation for multicarrier D2D video transmission is formulated, and an iterative subcarrier and power allocation algorithm is proposed. Section V presents the simulation results, and compares the performance of the proposed algorithm with the performance of the same algorithm using the SER obtained by the GA. Section VI contains the conclusion.

II. System Model

Consider a single cell D2D video transmission system served by a base station (BS). There are K pairs of D2D users in the cell. Each D2D pair consists of a transmitter and a receiver, with a D2D link from the transmitter to the receiver. The system allocates a total frequency band of W (Hz), which is equally divided into M_c orthogonal subcarriers, exclusively to these D2D pairs [29]. Every D2D pair has access to any of these subcarriers subject to the subcarrier and power allocation by the BS.

The system operates in a time-slot manner. We consider video delivery with a delay constraint, for which one group of pictures (GOP) is transmitted in each time slot. The duration of a GOP, denoted by T_{GOP}, is a constant. The subcarrier assignment and power allocation decision is made by the BS at the beginning of each GOP. We assume perfect channel estimation for the desired signal and interfering signals at receivers, and the BS is able to collect the channel state information (CSI) and video rate-distortion (RD) information via the control channels without error.

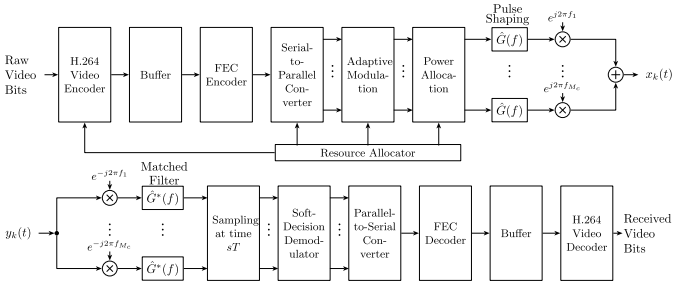

Fig. 1. Block diagram of the transceiver.

A. Transceiver Architecture

The transceiver adopts a multicarrier architecture, whose block diagrams are given in Fig. 1. The FEC protected video bit sequences are mapped to the subcarriers as complex-valued modulated symbol sequences at a symbol rate of $1/T$. The signal on the m-th subcarrier of the k-th transmitter is modulated by $M_{k,m}$-ary QAM, where the $\{\sqrt{M_{k,m}}\}$ are positive even integers. he s-th complex modulated symbol on the m-th subcarrier of the k-th transmitter is denoted by $X_k^{(m)}[s]$, where $\mathrm{Var}[X_k^{(m)}[s]] = E[|X_k^{(m)}[s]|]^2/2$ is normalized to unity. The transmitted pulse is denoted by $\hat{g}(t)$, whose energy is normalized to unity, i.e. $\int_{-\infty}^{\infty}[\hat{g}(t)]^2 = 1$. The lowpass equivalent signal for the k-th D2D transmitter is given by

$$x_k(t) = \sum_{m=1}^{M_c} \sqrt{p_{k,m}T} \sum_s X_k^{(m)}[s]\, \hat{g}(t - sT)\, e^{j2\pi f_m t}, \quad (1)$$

where $p_{k,m}$ is the transmission power on the m-th subcarrier of the k-th D2D transmitter, and the central frequency of the m-th subcarrier is denoted by $f_m = (m - 1/2)W/M_c$. Let the frequency response of $\hat{g}(t)$ be $\hat{G}(f)$. The cascade of the pulse shaping and matched filter $G(f) = |\hat{G}(f)|^2$ belongs to a parametric family of Nyquist pulses [30, 5(a)], given by

$$G(f) = \begin{cases} T, & 0 \le f \le \dfrac{1-\beta}{2T}, \\ T\,\mathcal{G}\left(\gamma_r \left[f - \dfrac{1-\beta}{2T}\right]^r\right), & \dfrac{1-\beta}{2T} < f \le \dfrac{1}{2T}, \\ T\left\{1 - \mathcal{G}\left(\gamma_r \left[\dfrac{1+\beta}{2T} - f\right]^r\right)\right\}, & \dfrac{1}{2T} < f \le \dfrac{1+\beta}{2T}, \\ 0, & f > \dfrac{1+\beta}{2T}, \end{cases} \quad (2)$$

where r is a positive, finite integer, $0 < \beta \le 1$, $\gamma_r \triangleq (2T/\beta)^r\, \mathcal{G}^{-1}(1/2)$, and $\mathcal{G}(f)$ is a continuous function that

possesses derivatives of all orders and satisfies $\mathcal{G}(0) = 1$. The pulse is conjugate symmetry in the frequency domain, namely $G(f) = G^*(-f)$. The conjugate frequency symmetry implies that the time pulse of $G(f)$, denoted by $g(t)$, is real valued. This parametric family of pulses in (2) includes many pulses that are candidates for next generation communications [31], such as the raised-cosine pulse [32], obtained by setting $r = 1$, $\gamma_r = \pi T/(2\beta)$ and $\mathcal{G}(f) = \cos^2(f)$, and the conjugate-root pulses [30], [33], obtained by setting $r = 1$, $\gamma_r = T/\beta$ with $\mathcal{G}(f) = \cos^2(\pi f/2)$ or $\mathcal{G}(f) = \cos^2[(\pi/2)f^4(35 - 84f + 70f^2 - 20f^3)]$. The bandwidth of $G(f)$ is $(1 + \beta)/(2T)$. The system adopts a FMT waveform [5], in which the spectra of adjacent subcarriers do not overlap, namely $(1 + \beta)/T \leq W/M_c$, so ICI does not exist. Since $G(f)$ is a Nyquist pulse, inter-symbol interference does not exist if there is perfect bit synchronization.

The interference from the i-th transmitter arrives at the k-th receiver with a channel gain of $|h_m^{i,k}|$, a time delay $\tau_i^{(k)}$ and a phase delay $\phi_i^{(k)}$ compared to the desired signal from the k-th transmitter ($i, k = 1, 2, \cdots, K$), where $\phi_i^{(k)}$ is uniformly distributed in $[0, 2\pi)$ and $\tau_i^{(k)}$ modulo T is uniformly distributed in $[0, T)$, if $i \neq k$. Also, $|\tau_i^{(k)}| \ll T_{\text{GOP}}$. We assume that a coherent receiver is implemented and the receiver maintains perfect bit synchronization and phase recovery for the desired signal, so we set $\tau_k^{(k)} = 0$ and $\phi_k^{(k)} = 0$. We further assume that the channel gain $|h_m^{i,k}|$ is unchanged for the duration of a time slot [18], [19]. Therefore, the lowpass equivalent signal at the k-th receiver is given by

$$y_k(t) = \sum_{m=1}^{M_c} \sum_{i=1}^{K} \sqrt{P_i^{(k,m)} T} \sum_s X_k^{(m)}[s]\, \hat{g}(t - \tau_i^{(k)} - sT) \cdot e^{j(2\pi f_m t + \phi_i^{(k)})} + n_k(t), \tag{3}$$

where $P_i^{(k,m)} = p_{i,m}|h_m^{i,k}|^2$ is the power of the i-th signal received on the m-th subcarrier of the k-th D2D receiver prior to demodulation, and $n_k(t)$ is complex Additive White Gaussian Noise (AWGN) at the k-th receiver with two-sided power spectral density N_0. As shown in Fig. 1, a matched filter is used at subcarrier m of the k-th receiver, so the output for the s-th symbol is given by $Y_k^{(m)}[s] = \int_{-\infty}^{\infty} y_k(t)\hat{g}(t - sT)\exp(-j2\pi f_m t)dt$. Without loss of generality, we consider the reception of the 0-th symbol. The decision statistic for the 0-th symbol at the output of the matched filter is given by

$$Y_k^{(m)}[0] = \sqrt{P_k^{(k,m)} T}\, X_k^{(m)}[0] + \sum_{i=1, i\neq k}^{K} \sqrt{P_i^{(k,m)} T}\, e^{j\phi_i^{(k)}} \cdot \sum_s X_i^{(m)}[s]\, g(-\tau_i^{(k)} - sT) + N_k^{(m)}[0]. \tag{4}$$

In (4), the first term is the desired signal component, and the second term represents the CCI components. The noise term is given by $N_k^{(m)}[s] = \int_{-\infty}^{\infty} n_w(t)\hat{g}(t - sT)dt$, which is a zero-mean complex circularly symmetric Gaussian (CCSG) random variable (RV) with power $P_N = N_0 \int_{-\infty}^{\infty}[\hat{g}(t)]^2 dt = N_0$. Therefore, the signal-to-noise power ratio (SNR) and the signal-to-interference power ratio (SIR) on the m-th subcarrier of the k-th D2D receiver can be expressed as $\text{SNR}_{k,m} = 10\log_{10}\left[p_{k,m}|h_m^{k,k}|^2/(N_0/T)\right]$ and $\text{SIR}_{k,m} = 10\log_{10}[p_{k,m}|h_m^{k,k}|^2/(\sum_{i=1,i\neq k}^{K} p_{i,m}|h_m^{i,k}|^2)]$.

B. Scalable Video Codec

The D2D videos are encoded with the scalable video coding extension of H.264/AVC with medium granular scalability (MGS) [34]. In each bitstream, the most important video information is conveyed by the base layer (BL), and other video information of diminishing importance is contained in the successive enhancement layers (ELs). With a scalable video codec, the decoder only needs a portion of the encoded bitstream to display the video. The decoded fidelity of the video depends on the length of the bitstream, as well as the rate distortion characteristics of the video content. The mean square error (MSE) of the video diminishes as more ELs are received. The video packets are transmitted in the order of descending priority. If an error occurs during transmission, that packet and all successive packets in the GOP will be dropped, but previous packets will be used for decoding the GOP.

The RD curve of the video characterizes the tradeoff between the video distortion and the number of bits used to compress the raw video data. Since the video is compressed on a GOP-by-GOP basis, this RD function is also measured for each GOP. The MSE distortion D_k can be approximated as a function of the number of correctly received video bits B_k in the GOP, written as [35]

$$D_k = a_k + \frac{b_k'}{B_k + c_k'}, \tag{5}$$

where a_k, b_k', and c_k' depend on video content and are positive constants determined by curve fitting. We assume that one GOP is transmitted in each time slot, thus the duration of a GOP (T_{GOP}) is equal to the duration of the time slot. The video bits are protected by a FEC code with fixed rate u. The number of coded bits per symbol transmitted on the m-th subcarrier of the k-th link is $\log_2(M_{k,m})$, if the modulation format is $M_{k,m}$-ary QAM. The number of video bits (B_k) transmitted on the k-th link in a time slot is given by

$$B_k = \frac{uT_{\text{GOP}}}{T} \sum_{m=1}^{M_c} \log_2(M_{k,m}). \tag{6}$$

For simplicity, define $b_k \triangleq b_k' T/(uT_{\text{GOP}})$, $c_k \triangleq c_k' T/(uT_{\text{GOP}})$. Substituting (6) into (5), the MSE of the GOP at the video decoder can be further written as

$$D_k = a_k + \frac{b_k}{\sum_{m=1}^{M_c} \log_2(M_{k,m}) + c_k}. \tag{7}$$

III. Symbol Error Rate for D2D Receivers

In this section, we consider the SER on the m-th subcarrier of the k-th D2D receiver. As a remark, in this section, we omit the indices m and k in the superscripts of variables for simplicity of notation unless otherwise stated.

The aggregated CCI in the decision statistic in (4) is denoted by $I = \sum_{i=1, i\neq k}^{K} I_i$, where the CCI from the i-th transmitter is given by

$$I_i = \sqrt{P_i T}\, e^{j\phi_i} \sum_{s=-\infty}^{\infty} X_i[s]\, g(-\tau_i - sT), \tag{8}$$

A. SER Evaluation by Gaussian Approximation for the CCI

The GA treats the aggregated CCI as a zero-mean circularly complex Gaussian RV with the same variance. Since $E(I_i) = 0$, we have $\mathrm{Var}(I_i) = E(|I_i|^2)/2$. The variance of the aggregated CCI is given by

$$\mathrm{Var}(I) = \sum_{i=1, i\neq k}^{K} \mathrm{Var}(I_i) = \sum_{i=1, i\neq k}^{K} \gamma\, P_i T, \tag{9}$$

where γ is defined by $\gamma \triangleq E\left[\sum_{s=-\infty}^{\infty} g^2(-\tau_i - sT)\right]$. Invoking the well-known Poisson summation formula [36, p. 47, (3-56)], γ is given by

$$\begin{aligned}\gamma &= E\left[\frac{1}{T}\sum_{n=-\infty}^{\infty} G_2\left(\frac{n}{T}\right) e^{jn\frac{2\pi\tau_i}{T}}\right] \\ &= \frac{G_2(0)}{T} = \frac{1}{T}\int_{-\infty}^{\infty} |G(f)|^2 df,\end{aligned} \tag{10}$$

where the Fourier transform of $g^2(t)$ is denoted by $G_2(f)$, which equals $G(f) * G(f)$, and $*$ stands for convolution. Specially, $\gamma = 1 - \beta/4$ for a raised-cosine pulse with roll-off factor β [9, eq. (55)].

With the GA, the SER evaluation for QAM in CCI plus AWGN resembles the well-known SER expression in AWGN [37], which depends on the signal-to-interference-plus-noise ratio (SINR). The SER of $M_{k,m}$-ary QAM under the CCI using the GA is thus given by

$$\begin{aligned}\mathrm{SER}_{k,m}^{\mathrm{GA}} &= 4\left(1 - \frac{1}{\sqrt{M_{k,m}}}\right) Q\left(\sqrt{\frac{3\,\mathrm{SINR}_{k,m}}{M_{k,m}-1}}\right) \\ &\quad - 4\left(1 - \frac{1}{\sqrt{M_{k,m}}}\right)^2 Q^2\left(\sqrt{\frac{3\,\mathrm{SINR}_{k,m}}{M_{k,m}-1}}\right),\end{aligned} \tag{11}$$

where the received SINR is given by

$$\mathrm{SINR}_{k,m} = \frac{p_{k,m}|h_m^{k,k}|^2}{\gamma \sum_{i=1, i\neq k}^{K} p_{i,m}|h_m^{i,k}|^2 + N_0/T}. \tag{12}$$

B. Characteristic Function of the CCI

To demonstrate the inaccuracy of the GA in the evaluation of the SER for multicarrier D2D systems, we derive the exact expression for the SER of the bandlimited QAM under CCI and AWGN. We start with the characteristic function (CF) of the CCI. The minimum distance between two adjacent constellation points of the i-th QAM signal at the k-th D2D receiver is denoted by $2A_i$. Since P_i is the power of the i-th QAM signal at the receiver, A_i is given by [13, eq. (19)]

$$A_i = \sqrt{\frac{3P_iT}{M_{i,m}-1}}. \tag{13}$$

We also denote the in-phase and quadrature components of the i-th CCI signal by $I_i^I = \mathrm{Re}(I_i)$ and $I_i^Q = \mathrm{Im}(I_i)$. To derive the joint CF of I_i^I and I_i^Q, we first consider their conditional joint CF, given ϕ_i and τ_i, which is presented in Proposition 1.

Proposition 1: Given τ_i and ϕ_i, the conditional joint CF of I_i^I and I_i^Q is given by (14), as shown at the bottom of this page.

Proof: See Appendix A. ∎

Averaging over ϕ_i and τ_i, the joint CF of I_i^I and I_i^Q is given by

$$\varphi_{I_i^I, I_i^Q}(u,v) = \frac{1}{2\pi T}\int_0^T \int_0^{2\pi} \varphi_{I_i^I, I_i^Q|\tau_i,\phi_i}(u,v|\tau_i,\phi_i)\, d\phi_i d\tau_i. \tag{15}$$

Using the assumption that all CCI signals are independent and $I^I = \sum_{i=1, i\neq k}^{K} I_i^I$, $I^Q = \sum_{i=1, i\neq k}^{K} I_i^Q$, the joint CF of the in-phase and the quadrature components of the aggregated CCI is given by

$$\varphi_{I^I, I^Q}(u,v) = \prod_{i=1, i\neq k}^{K} \varphi_{I_i^I, I_i^Q}(u,v). \tag{16}$$

Substituting (14) and (15) into (26), the CF of the aggregated CCI can be obtained in an integral form. However, the integral in (15) does not appear to have a closed-form expression due to the implicit dependence on the pulse shape. To evaluate an integral with this form, [9] numerically integrates the result without providing an analytical expression for the error rate. In contrast, the analysis in this paper proceeds by expanding $\varphi_{I_i^I, I_i^Q}(u,v)$ in a power series, averaging over τ_i, ϕ_i term by term, and finally deriving an analytical expression for the error rate in the form of a power series. The convergence analysis for the resulting power series is also provided in a later section.

$$\begin{aligned}\varphi_{I_i^I, I_i^Q|\tau_i,\phi_i}(u,v|\tau_i,\phi_i) &= \prod_{s_1=-\infty}^{\infty} \frac{2}{\sqrt{M_{i,m}}} \sum_{j_1=1}^{\sqrt{M_{i,m}}/2} \cos\Big(A_i(u\cos\phi_i + v\sin\phi_i)(2j_1-1)g(-\tau_i - s_1T)\Big) \\ &\quad \cdot \prod_{s_2=-\infty}^{\infty} \frac{2}{\sqrt{M_{i,m}}} \sum_{j_2=1}^{\sqrt{M_{i,m}}/2} \cos\Big(A_i(v\cos\phi_i - u\sin\phi_i)(2j_2-1)g(-\tau_i - s_2T)\Big).\end{aligned} \tag{14}$$

We present in Proposition 2 a power series expansion for the joint CF of the in-phase and quadrature components of the aggregated CCI.

Proposition 2: The power series expansion of the joint CF of I^I and I^Q is given by

$$\varphi_{I^I,I^Q}(u,v)=\sum_{n=0}^{\infty} b_n^{(k,m)}(-N_0)^n(u^2+v^2)^n, \tag{17}$$

where $b_0^{(k,m)}=1$ and a recursive relation of $b_n^{(k,m)}$ for any positive integer n is given by

$$b_n^{(k,m)}=\sum_{p=1}^{n}\frac{p}{n}b_{n-p}^{(k,m)}\sum_{i=1,i\neq k}^{K}\left(\frac{P_i^{(k,m)}T}{N_0}\right)^p d_p^{(M_{i,m})}. \tag{18}$$

In (18), $d_0^{(M_{i,m})}=0$ and the following recursive relationship holds for any positive integer n:

$$d_n^{(M_{i,m})}=\alpha_n^{(M_{i,m})}-\sum_{p=1}^{n-1}\frac{p}{n}d_p^{(M_{i,m})}\alpha_{n-p}^{(M_{i,m})}, \tag{19}$$

where the $\{\alpha_n^{(M_{i,m})}\}$ are the coefficients of the power series by expanding the joint CF of I_i^I and I_i^Q, i.e., $\varphi_{I_i^I,I_i^Q}(u,v)=\sum_{n=0}^{\infty}\alpha_n^{(M_{i,m})}[-P_i^{(k,m)}T(u^2+v^2)]^n$. The expression for $\{\alpha_n^{(M)}\}$, as a function of alphabet size M, is given by

$$\begin{aligned}\alpha_n^{(M)}&=\left(\frac{3}{M-1}\right)^n\sum_{p=0}^{n}B_{2p,2(n-p)}\sum_{q=0}^{2n}\sum_{q_1=0}^{q}B_{q_1,q-q_1}\sum_{q_2=\max(0,q+2p-2n)}^{\min(q,2p)}\\&\quad\cdot\sum_{q_3=\max(0,q_1+q_2-q)}^{\min(q_1,q_2)}w_p^{(M)}(q_2,q_3)w_{n-p}^{(M)}(q-q_2,q_1-q_3),\end{aligned} \tag{20}$$

where $B_{m,n}=(m-1)!!\,(n-1)!!/[(m+n)!!]$ if $m\geq 0$, $n\geq 0$, m,n are both even, and $B_{m,n}=0$ otherwise. $(2n-1)!!=1\cdot 3\cdots(2n-1)$, $(2n)!!=2\cdot 4\cdots 2n$ for any positive integer n, and $0!!=(-1)!!=1$.

For $n\geq 1$, $0\leq q_1\leq q\leq 2n$, the coefficients $\{w_n^{(M)}(q,q_1)\}$ in (20) are given by

$$\begin{aligned}w_n^{(M)}(q,q_1)&=\sum_{p=1}^{n}\frac{p}{n}c_p^{(M)}\sum_{q_2=\max(0,q+2p-2n)}^{\min(q,2p)}\\&\quad\cdot\sum_{q_3=\max(0,q_1+q_2-q)}^{\min(q_1,q_2)}R_p(q_2,q_3)w_{n-p}^{(M)}(q-q_2,q_1-q_3),\end{aligned} \tag{21}$$

where the initial condition is given by $w_0^{(M)}(0,0)=1$, and the $\{c_n^{(M)}\}$ are given by $c_0^{(M)}=0$ and $c_n^{(M)}=a_n^{(M)}-\sum_{p=1}^{n-1}(p/n)c_p^{(M)}a_{n-p}^{(M)}$ for $n=1,2,\cdots$, where the $\{a_n^{(M)}\}$ are given by $a_n^{(M)}=2/[(2n)!\sqrt{M}]\sum_{l=1}^{\sqrt{M}/2}(2l-1)^{2n}$.

Lastly, the $\{R_n(s,s_1)\}$ in (21) are defined by

$$R_n(s,s_1)=\begin{cases}\dfrac{2-\delta_s}{T}\mathrm{Re}\left[G_{2n}\left(\dfrac{s}{T}\right)\right]\dbinom{s}{s_1}(-1)^{s_1/2},\\ \qquad\text{if } s_1 \text{ even},\quad 0\leq s_1\leq s\leq 2n,\\ \dfrac{2}{T}\,\mathrm{Im}\left[G_{2n}\left(\dfrac{s}{T}\right)\right]\dbinom{s}{s_1}(-1)^{(s_1+1)/2},\\ \qquad\text{if } s_1 \text{ odd},\quad 0\leq s_1\leq s\leq 2n,\\ 0,\qquad\text{otherwise},\end{cases} \tag{22}$$

where the Fourier transform of $[g(t)]^{2n}$ is denoted by $G_{2n}(f)=\int_{-\infty}^{\infty}[g(t)]^{2n}\exp(j2\pi ft)\,dt$, and δ_s is the Kronecker delta function.

Proof: See Appendix B. ∎

Among the coefficients in Proposition 2, only $\{b_n^{(k,m)}\}$ need to be calculated online using (18). The other coefficients are determined by the alphabet size and pulse shape but do not depend on the signal power, and can be calculated offline.

C. Exact SER in the Form of a Power Series

We use Proposition 2 to derive the exact expression for the SER. The in-phase and quadrature components of the noise in the decision statistics are denoted by $n^I=\mathrm{Re}(N_k[0])$ and $n^Q=\mathrm{Im}(N_k[0])$. Let the sum of the aggregated CCI and the noise be $Z=I+N_k[0]$. We also denote $I^I=\mathrm{Re}(I)$, $I^Q=\mathrm{Im}(I)$, $Z^I=\mathrm{Re}(Z)=I^I+n^I$ and $Z^Q=\mathrm{Im}(Z)=I^Q+n^Q$. The event that Z^I and Z^Q both fall in the range $(-A_k,A_k)$ is denoted by $\mathcal{B}_1$, whose probability is written as

$$\Pr(\mathcal{B}_1)=\Pr(|Z^I|<A_k,|Z^Q|<A_k). \tag{23}$$

Let $\mathcal{B}_2$ be the event that Z^I falls in the range $(-A_k,A_k)$, whose probability is given by

$$\Pr(\mathcal{B}_2)=\Pr(|Z^I|<A_k). \tag{24}$$

We see from (8) that the CCI in the decision statistics is a complex circularly symmetric RV, since the phase shifts $\{\phi_i\}$ are assumed to be uniformly distributed in $[0,2\pi)$. Also recall that the noise $N_w[0]$ is a complex circularly symmetric RV. Therefore, $Z=I+N_k[0]$ is a complex circularly symmetric RV. Making use of the circular symmetry of Z, the constellation points of the transmitted desired signal can be classified into three categories [14]: 1) points at the four corners; 2) points at the edge of the constellation but not corners; 3) interior points. We denote the event of the transmitted symbol being in Category 1, 2 and 3 by $\mathcal{C}_1$, $\mathcal{C}_2$ and $\mathcal{C}_3$, respectively. Let c be the event of a symbol being correctly received. Making use of the circular symmetry of Z, the expressions for $\{\Pr(c|\mathcal{C}_j)\}$ are given by

$$\begin{aligned}\Pr(c|\mathcal{C}_1)&=\Pr(Z^I<A_k,Z^Q<A_k)=\frac{1}{4}+\frac{1}{4}\Pr(\mathcal{B}_1)+\frac{1}{2}\Pr(\mathcal{B}_2),\\ \Pr(c|\mathcal{C}_2)&=\Pr(Z^I<A_k,|Z^Q|<A_k)=\frac{1}{2}\Pr(\mathcal{B}_1)+\frac{1}{2}\Pr(\mathcal{B}_2),\\ \Pr(c|\mathcal{C}_3)&=\Pr(|Z^I|<A_k,|Z^Q|<A_k)=\Pr(\mathcal{B}_1).\end{aligned} \tag{25}$$

Since each constellation point is assumed to appear with equal probability, we obtain $\Pr(\mathcal{C}_1)=4/M_{k,m}$,

$\Pr(\mathcal{C}_2) = 4(\sqrt{M_{k,m}}-1)/M_{k,m}$ and $\Pr(\mathcal{C}_3) = (\sqrt{M_{k,m}}-2)^2/M_{k,m}$. The SER is thus given by

$$\begin{aligned}\mathrm{SER}_{k,m} &= 1-\sum_{j=1}^{3}\Pr(\mathcal{C}_j)\cdot\Pr(c|\mathcal{C}_j)\\ &= 1-\frac{(\sqrt{M_{k,m}}-1)^2\Pr(\mathcal{B}_1)+2(\sqrt{M_{k,m}}-1)\Pr(\mathcal{B}_2)+1}{M_{k,m}}.\end{aligned} \tag{26}$$

Invoking [38, p. 101, eq. (10.6.2)], we have

$$\begin{aligned}&\Pr(|Z^I|<A_k,|Z^Q|<A_k)\\ &\quad=\frac{1}{\pi^2}\int_{-\infty}^{\infty}\int_{-\infty}^{\infty}\frac{\sin(A_k u)}{u}\frac{\sin(A_k v)}{v}\varphi_{Z^I,Z^Q}(u,v)\,du dv,\end{aligned} \tag{27}$$

where the joint CF of Z^I, Z^Q is given by $\varphi_{Z^I,Z^Q}(u,v) = \varphi_{I^I,I^Q}(u,v)\varphi_{n^I,n^Q}(u,v)$, since the interference and noise are independent. Also, the joint CF of n^I and n^Q is $\varphi_{n^I,n^Q}(u,v) = \exp[-N_0(u^2+v^2)/2]$ since n^I, n^Q are i.i.d zero-mean jointly Gaussian RVs with variance N_0. Substituting (17) and (27) into (23) yields

$$\begin{aligned}\Pr(\mathcal{B}_1) = \frac{1}{\pi^2}\int_{-\infty}^{\infty}\int_{-\infty}^{\infty}\frac{\sin(A_k u)}{u}\frac{\sin(A_k v)}{v}e^{-\frac{N_0(u^2+v^2)}{2}}\\ \cdot\left[\sum_{n=0}^{\infty}b_n^{(k,m)}(-N_0)^n(u^2+v^2)^n\right]du dv.\end{aligned} \tag{28}$$

Using the binomial theorem to expand $(u^2+v^2)^n$, (28) can be rewritten as

$$\begin{aligned}\Pr(\mathcal{B}_1) =& \sum_{n=0}^{\infty}\sum_{p=0}^{n}\frac{b_n^{(k,m)}(-N_0)^n}{\pi^2}\binom{n}{p}\\ &\cdot\int_{-\infty}^{\infty}\sin(A_k u)u^{2p-1}e^{-\frac{u^2N_0}{2}}du\\ &\cdot\int_{-\infty}^{\infty}\sin(A_k v)v^{2(n-p)-1}e^{-\frac{v^2N_0}{2}}dv.\end{aligned} \tag{29}$$

From [39, 3.952 (6)] and [39, 3.952 (10)], respectively, we obtain $\int_{-\infty}^{\infty}\sin(A_k u)u^{-1}\exp(-u^2N_0/2)\,du = \pi[1-2Q(A_k/\sqrt{N_0})]$ and $\int_{-\infty}^{\infty}\sin(A_k u)u^{2l-1}\exp(-u^2N_0/2)\,du = (-1)^{l-1}(2\sqrt{\pi}/N_0{}^l)\exp[-A_k^2/(2N_0)]H_{2l-1}(A_k/\sqrt{2N_0})$ for positive integer l, where $H_n(x)$ is the Hermite polynomial of the n-th order with the following recursive relation [39, 8.95]: $H_0(x)=1$, $H_1(x)=2x$, and for $n=2,3,\cdots$:

$$H_{n+1}(x) = 2xH_n(x) - 2nH_{n-1}(x). \tag{30}$$

Therefore, (29) reduces to

$$\begin{aligned}\Pr(\mathcal{B}_1) =& \left[1-2Q\left(\frac{A_k}{\sqrt{N_0}}\right)\right]^2 - \frac{4}{\sqrt{\pi}}\left[1-2Q\left(\frac{A_k}{\sqrt{N_0}}\right)\right]e^{-\frac{A_k^2}{2N_0}}\\ &\cdot\sum_{l=1}^{\infty}b_l^{(k,m)}H_{2l-1}\left(\frac{A_k}{\sqrt{2N_0}}\right)+\frac{4}{\pi}e^{-\frac{A_k^2}{N_0}}\sum_{n=1}^{\infty}\sum_{p=1}^{n-1}b_n^{(k,m)}\\ &\cdot\binom{n}{p}H_{2p-1}\left(\frac{A_k}{\sqrt{2N_0}}\right)H_{2(n-p)-1}\left(\frac{A_k}{\sqrt{2N_0}}\right).\end{aligned} \tag{31}$$

Using a similar procedure, and applying [38, p. 101, eq. (10.6.2)] to (24), $\Pr(\mathcal{B}_2)$ is given by

$$\begin{aligned}\Pr(\mathcal{B}_2) = \Pr\left(\left|Z^I\right|<A_k\right) &= \frac{1}{\pi}\int_{-\infty}^{\infty}\frac{\sin(A_k u)}{u}\varphi_{Z^I}(u)\,du\\ &= \frac{1}{\pi}\int_{-\infty}^{\infty}\frac{\sin(A_k u)}{u}\varphi_{I^I,I^Q}(u,0)e^{-\frac{u^2N_0}{2}}du\\ &= \frac{1}{\pi}\int_{-\infty}^{\infty}\frac{\sin(A_k u)}{u}\left[\sum_{l=0}^{\infty}b_l^{(k,m)}(-N_0)^l u^{2l}\right]e^{-\frac{u^2N_0}{2}}du,\end{aligned} \tag{32}$$

where the third equality is due to $\varphi_{I^I}(u) = E\{\exp[j(uI^I + vI^Q)]\}|_{v=0} = \varphi_{I^I,I^Q}(u,0)$. Similarly, (32) reduces

$$\begin{aligned}\Pr(\mathcal{B}_2) =& 1-2Q\left(\frac{A_k}{\sqrt{N_0}}\right)\\ &-\frac{2}{\sqrt{\pi}}e^{-\frac{A_k^2}{2N_0}}\sum_{l=1}^{\infty}b_l^{(k,m)}H_{2l-1}\left(\frac{A_k}{\sqrt{2N_0}}\right).\end{aligned} \tag{33}$$

Substituting (31) and (33) into (26), after some manipulations and denoting $\nu_{k,m} \triangleq A_{k,m}/\sqrt{2N_0} = \{3p_{k,m}|h_m^{k,k}|^2T/[2N_0(M_{k,m}-1)]\}^{1/2}$, $\mu_{k,m} \triangleq 1-1/\sqrt{M_{k,m}}$, the exact SER on the m-th subcarrier of the k-th D2D receiver is given by $\mathrm{SER}_{k,m}^{\mathrm{exact}} = \mathrm{SER}_{k,m}^{(\infty)} = \lim_{L\to\infty}\mathrm{SER}_{k,m}^{(2L)}$, where $\mathrm{SER}_{k,m}^{(2L)}$ is given by (34), as shown at the bottom of this page, and the coefficients $\{b_n^{(k,m)}\}$ are given in (18). If CCI is absent, then $b_n^{(k,m)}=0$ for $n=1,2,\cdots$, thereby reducing (34) to the SER for $M_{k,m}$-ary QAM in AWGN [37].

In practice, we only use a finite number of terms from the power series of the CF of CCI to calculate the SER. Retaining the terms with order less than $2L$ from $\varphi_{I^I,I^Q}(u,v)$ in the evaluation of the SER, where L is a positive integer, one can formally define the truncated evaluation for SER as (34).

By comparing $\mathrm{SER}_{k,m}^{(2L)}$ in (34) and $\mathrm{SER}_{k,m}^{\mathrm{exact}}$, a truncation error is introduced. We denote the truncation error by $e(2L) = |\mathrm{SER}_{k,m}^{\mathrm{exact}} - \mathrm{SER}_{k,m}^{(2L)}|$. Appendix C gives an upper bound for

$$\begin{aligned}\mathrm{SER}_{k,m}^{(2L)} =& 4\mu_{k,m}Q(\sqrt{2}\nu_{k,m}) - 4\mu_{k,m}^2\left[Q(\sqrt{2}\nu_{k,m})\right]^2 + \frac{4\mu_{k,m}}{\sqrt{\pi}}e^{-\nu_{k,m}^2}\left[1-2\mu_{k,m}Q(\sqrt{2}\nu_{k,m})\right]\sum_{l=1}^{L-1}b_l^{(k,m)}H_{2l-1}(\nu_{k,m})\\ &-\frac{4\mu_{k,m}^2}{\pi}e^{-2\nu_{k,m}^2}\sum_{n=1}^{L-1}\sum_{p=1}^{n-1}b_n^{(k,m)}\binom{n}{p}H_{2p-1}(\nu_{k,m})H_{2(n-p)-1}(\nu_{k,m}),\end{aligned} \tag{34}$$

the truncation error in (C.12), which is repeated below:

$$e(2L) < \frac{1}{M_{k,m}}\sqrt{\frac{6p_{k,m}|h_m^{k,k}|^2}{\pi N_0/T}}\left(C\sum_{i=1,i\neq k}^{K}\sqrt{\frac{6p_{i,m}|h_m^{i,k}|^2}{N_0/T}}\right)^{2L} \cdot\left(\sqrt{\frac{6p_{k,m}|h_m^{k,k}|^2}{\pi N_0/T}}\frac{1}{(2L-1)!!}+\frac{2}{(2L)!!}\right), \quad (35)$$

where L is a positive integer, and $C = \sup_{0<\tau<T}\{\sum_{s=-\infty}^{\infty}|g(\tau - sT)|\}$. Using the results in [30], the constant C can be shown to be finite for the family of Nyquist pulses that are considered in (2). For example, $C = 10\sqrt{2}/(3\pi) \approx 1.5005$ for a raised-cosine pulse with roll-off factor $\beta = 0.5$, given by Proposition 3 in Appendix C. Notice that $e(2L) \to 0$ as $L \to \infty$. Therefore, the truncated series in (34) converges to the exact SER as more terms are used in the calculation.

IV. Iterative Cross-layer Resource Allocation Algorithm

We formulate the optimization problem for resource allocation in multicarrier D2D video transmission system, and propose an iterative algorithm for subcarrier assignment and power allocation.

A. Problem Formulation

The objective for resource allocation is to minimize the total video MSE for all D2D pairs. The BS collects the RD information and the channel conditions of all D2D pairs, and allocates subcarriers and transmission power to D2D pairs based on both the RD functions and channel conditions.

Recall that the transmission power and the alphabet size of the k-th D2D pair on subcarrier m are denoted by $p_{k,m}$ and $M_{k,m}$, respectively. We denote the number of supported alphabet sizes by N_A and the set of supported alphabet sizes by $\mathcal{M}_{\mathcal{A}} = \{\mathcal{M}_1, \cdots, \mathcal{M}_{N_A}\}$, where $\mathcal{M}_1 < \mathcal{M}_2 < \cdots < \mathcal{M}_{N_A}$. We only consider square QAM in this paper, so the number of bits per symbol ($\log_2(\mathcal{M}_n)$) is a non-negative even integer. We set $\mathcal{M}_1 = 1$, which indicates that the number of bits per symbol is $\log_2(\mathcal{M}_1) = 0$ and corresponds to the case of no transmission.

Each D2D transmitter is subject to a total power constraint P. In the search procedure, the BS sets a fixed target for the SER on every D2D link and assumes error-free transmission in the power allocation algorithm if the SER target is satisfied.[1] The video MSE minimization problem is formally written as

$$\begin{aligned}&\text{minimize} \sum_{i=1,\, i\neq k}^{K}\frac{b_k}{\sum_{m=1}^{M_c}\log_2(M_{k,m})+c_k}\\ &\text{subject to (C1)} \sum_{m=1}^{M_c}p_{k,m}\le P,\ \forall k\in\{1,2,\cdots,K\},\\ &\quad\text{(C2) } \mathrm{SER}_{k,m}\le \mathrm{SER}_{\text{target}},\quad p_{k,m}\ge 0,\ M_{k,m}\in\mathcal{M}_A,\\ &\quad\forall k\in\{1,2,\cdots,K\},\quad \forall m\in\{1,2,\cdots,M_c\}.\end{aligned} \quad (36)$$

[1]This error-free assumption is only used in determining the subcarrier assignment and power allocation. In the simulation, an error may still occur even if the SER target is satisfied.

We omit the $\{a_k\}$ in (36), since $\{a_k\}$ are constant terms in the objective function for optimization. The constraint (C1) is the total power constraint for each D2D transmitter, and (C2) is the SER constraint for each subcarrier of each D2D pair that is demanded by video delivery with no retransmission. Since constraint (C2) is not a convex set and the optimization problem in (36) is NP-hard, we propose an iterative algorithm as a suboptimal solution, which updates both the subcarrier assignments and the power allocation strategy based on the CSI and the RD function. The details of the proposed algorithm are given in the next section.

B. Proposed Iterative Resource Allocation Algorithm

Our proposed algorithm is initialized by multi-user diversity (MUD), where each subcarrier is assigned to the D2D pair with the best channel gain. Next, we consider the D2D pair which has the steepest slope on the RD curve, and attempt to assign one additional subcarrier to this chosen D2D pair. The next step is to iterate over all subcarriers and iterate over all supported alphabet sizes for the chosen D2D pair. In the iteration, the minimal transmission power of the chosen D2D pair is calculated for each supported alphabet size on the current subcarrier via a bisection search, using either the proposed SER expression (34) or the SER obtained by the GA (11). For other D2D pairs on the current subcarrier, we also run an exhaustive search based on (34) or (11) for the largest alphabet sizes that satisfy the SER target under the interference from the chosen D2D pair. Afterwards, if the total MSE decreases, and the total transmission power of the chosen D2D pair does not exceed the power constraint, we update the transmission power, alphabet sizes and subcarrier assignment. This procedure is repeated iteratively until the total MSE of the video will not decrease by assigning one more subcarrier to any D2D pair.

The following notation will be used in the algorithm.

1) Let $\sigma_m^{(l)}$ be the set of D2D pairs that are allocated with subcarrier m in the l-th iteration;
2) The potential set $\Omega^{(l)}$ is the set of D2D pairs that are still possible to decrease the total video MSE by receiving an additional subcarrier at the l-th iteration.
3) $p_{k,m}^{(l)}$ and $M_{k,m}^{(l)}$ are the transmission power and alphabet size on subcarrier m of the k-th D2D pair at the l-th iteration, respectively.

The details of our proposed algorithm are elaborated as follows.

1) Initialization: The potential set $\Omega^{(0)}$ is initialized as the set of indices of all D2D pairs, i.e. $\Omega^{(0)} = \{1, 2, \cdots, K\}$. We first assign each subcarrier to the D2D pair who has the best channel response, i.e., $\sigma_m^{(0)} = \{\arg\max_{k\in\Omega^{(0)}}(h_m^{k,k})\}$ for $m = 1, 2, \cdots, M_c$. After the initial subcarrier assignment, each D2D pair maximizes its own bit rate by the conventional water-filling power allocation [26], namely $\hat{p}_{k,m} = \left[1/\lambda_k - 1/(\eta|h_m^{k,k}|^2)\right]^+$, where $\eta = (3/N_0)[Q^{-1}(\mathrm{SER}_{\text{target}}/4)]^{-2}$ [26] and $[x]^+ = \max(x, 0)$. The parameters $\{\lambda_k\}$ can be found numerically such that the total transmission power of each D2D pair is equal to the power

constraint, i.e., $\sum_{m=1}^{M_c} \hat{p}_{k,m} = P$. Given the water-filling power allocation, the alphabet sizes for initialization are given by [26, eq. (4)]:

$$M_{k,m}^{(0)} = \min\left(4^{\left\lfloor \log_4(1+\eta \hat{p}_{k,m}|h_m^{k,k}|^2)\right\rfloor}, \mathcal{M}_{N_A}\right), \tag{37}$$

where $\mathcal{M}_{N_A}$ is the largest alphabet size supported by the system. The transmission power is initialized as the minimal transmission power for alphabet size $M_{k,m}^{(0)}$, given by

$$p_{k,m}^{(0)} = \frac{M_{k,m}^{(0)} - 1}{\eta |h_m^{k,k}|^2}. \tag{38}$$

The iteration indicator l is initialized as $l = 0$.

2) Slope Calculation: The slope of the RD curve of the k-th D2D pair is given by

$$S_k^{(l)} = -\frac{c_k}{(\sum_{m=1}^{M_c} \log_2(M_{k,m}^{(l)}) + b_k)^2}. \tag{39}$$

In the l-th iteration, the index of the D2D pair with the steepest slope in the potential set ($\Omega^{(l)}$) is

$$k^* = \arg \min_{k \in \Omega^{(l)}} \{S_k^{(l)}\}. \tag{40}$$

We iterate over the subcarriers that are not currently allocated to D2D pair k^*, and denote the subcarrier index in the iteration by m^*. Note that m^* is only a candidate, and the decision for subcarrier assignment is not made until Step 4.

3) Video MSE Calculation: In this step, we let the alphabet size on the current subcarrier m^* of the k^*-th D2D pair iterate over the set of all supported alphabet sizes ($\mathcal{M}_{\mathcal{A}}$). We consider each supported modulation format $A_n \in \mathcal{M}_{\mathcal{A}}$, where $n = 1, 2, \cdots, N_A$. For the n-th supported alphabet size ($\mathcal{M}_n$), a minimal transmission power for D2D pair k^* on subcarrier m^*, denoted by $p_{k^*,m^*}[n]$, is calculated by a bisection search using either the proposed SER expression (34) or the SER under the GA (11), corresponding to interference power $\{p_{j,m^*}^{(l)}\}$, where $j \in \sigma_{m^*}^{(l)}$. Due to the interference caused by the newly added transmission power ($p_{k^*,m^*}[n]$) from the k^*-th D2D pair, the alphabet sizes of D2D pairs in set $\sigma_{m^*}^{(l)}$ on subcarrier m^* are updated as $\{\hat{M}_{j,m^*}[n]\}$, where $j \in \sigma_{m^*}^{(l)}$, via an exhaustive search within $\mathcal{M}_{\mathcal{A}}$ using either the proposed SER expression (34) or the SER under the GA (11).

Notice that the alphabet sizes of all D2D pairs that are assigned to subcarrier m^* and the k^*-th D2D pair are subject to change in the iterative search procedure. If the n-th supported alphabet size $\mathcal{M}_n$ is allocated to subcarrier m^* of D2D pair k^* as $\hat{M}_{k^*,m^*}[n] = \mathcal{M}_n$, the corresponding total video MSE is given by

$$\begin{aligned}\mathrm{MSE}_{\mathrm{total}}^{(l)}[n] &= \sum_{j \in \sigma_{m^*}^{(l)} \cup k^*} \frac{c_j}{\log_2(\hat{M}_{j,m^*}[n]) + \sum_{\substack{m=1 \\ m \neq m^*}}^{M_c} \log_2(M_{j,m}^{(l)}) + b_j} \\ &\quad + \sum_{k=1,\ k \notin \{\sigma_{m^*}^{(l)} \cup k^*\}}^{K} \frac{c_k}{\sum_{m=1}^{M_c} \log_2(M_{k,m}^{(l)}) + b_k}.\end{aligned} \tag{41}$$

This step will be repeated for each supported alphabet size, i.e., $n = 1, 2, \cdots, N_A$.

4) Subcarrier and Power Allocation: This step aims to determine whether the total video MSE will decrease by allocating D2D pair k^* with subcarrier m^* and to make the subcarrier assignment and power allocation decision for the $(l+1)$-th iteration. Among all supported modulation formats on subcarrier m^* of D2D pair k^*, the index of the modulation format that leads to the minimal total MSE is given by

$$n^* = \arg \min_{n \in \{1,2,\cdots,N_A\}} \mathrm{MSE}_{\mathrm{total}}^{(l)}[n], \tag{42}$$

where $\mathrm{MSE}_{\mathrm{total}}^{(l)}[n]$ is given by (41). We check whether the minimal total MSE is smaller than the total MSE at the start of the l-th iteration, namely $\mathrm{MSE}_{\mathrm{total}}^{(l)}[n^*] < \sum_{k=1}^{K} c_k / [\sum_{m=1}^{M_c} \log_2(M_{k,m}^{(l)}) + b_k]$, and check if the k^*-th D2D pair satisfies the total power constraint, namely $\sum_{m=1, m \neq m^*}^{M_c} p_{k^*,m}^{(l)} + p_{k^*,m^*}[n] \leq P$.

If both conditions are satisfied, then we assign D2D pair k^* to subcarrier m^* with alphabet size $\mathcal{M}_{n^*}$. Let $\sigma_{\mathrm{req}} = \{k \mid M_{k,m^*}[n^*] = \mathcal{M}_1,\ k \in \sigma_{m^*}^{(l)}\}$ be the indices of the D2D pairs that were previously allocated to subcarrier m^* whose alphabet size becomes $\mathcal{M}_1$. We let D2D pairs in σ_{req} relinquish subcarrier m^* and set their transmission power on subcarrier m^* to zero. We allocate the corresponding transmission power and alphabet sizes to D2D pairs $\sigma_{m^*}^{(l)}$ and D2D pair k^* for the next iteration. The specific update procedure is as follows,

$$p_{k,m}^{(l+1)} = \begin{cases} p_{k,m^*}[n^*], & \text{if } m = m^*,\ k = k^* \\ 0, & \text{if } m = m^*,\ k \in \sigma_{\mathrm{req}} \\ p_{k,m}^{(l)}, & \text{otherwise,} \end{cases} \tag{43a}$$

$$M_{k,m}^{(l+1)} = \begin{cases} \hat{M}_{k,m}[n^*], & \text{if } m = m^*,\ k \in \sigma_{m^*}^{(l)} \cup k^* \\ M_{k,m}^{(l)}, & \text{otherwise,} \end{cases} \tag{43b}$$

$$\sigma_{m^*}^{(l+1)} = (\sigma_{m^*}^{(l)} \cup k^*) \backslash \sigma_{\mathrm{req}}, \tag{43c}$$

$$\Omega^{(l+1)} = \Omega^{(l)} \cup \sigma_{\mathrm{req}}. \tag{43d}$$

Otherwise, we remove index k^* from the potential set by letting $\Omega^{(l+1)} = \Omega^{(l)} \backslash k^*$, and keep the power and alphabet sizes the same for the next iteration, namely $p_{k,m}^{(l+1)} = p_{k,m}^{(l)}$, $M_{k,m}^{(l+1)} = M_{k,m}^{(l)}$, $\sigma_{m^*}^{(l+1)} = \sigma_{m^*}^{(l)}$.

5) Termination: If the potential set Ω is not empty, the iteration indicator l is incremented by 1 and the algorithm returns to Step 2. Otherwise, the algorithm terminates.

As a summary, to compare the proposed SER expression (34) and the SER obtained by the GA (11) for resource allocation, the majority of the proposed algorithm is kept the same. Each of these two SER evaluation methods is applied in the bisection search for the minimal transmission power and the exhaustive search for the largest alphabet size in Step 3.

V. Results and Discussion

A. Numerical Results for the SER of a D2D Receiver

In this section, we investigate the SER of D2D receivers in CCI using the proposed exact SER expression. First, the proposed SER expression is corroborated by simulation. Next, we consider the SER under multiple interferers of equal received interference power. We then investigate the impact of a dominant interferer on the SER. Finally, we assess the

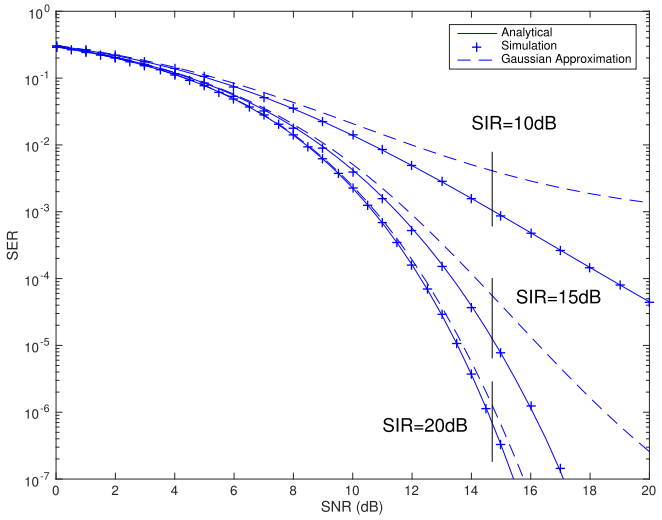

Fig. 2. SER versus SNR for the 4-QAM desired signal and one 16-QAM CCI signal at SIR= 10dB, 15dB and 20dB.

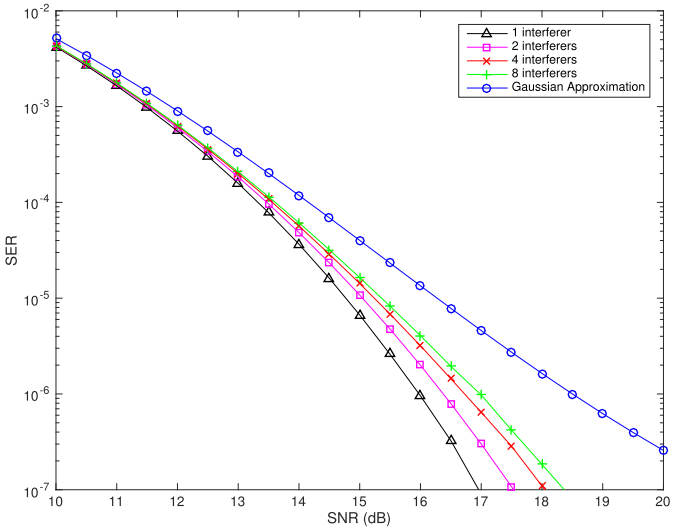

Fig. 3. SER versus SNR for one interferer and multiple interferers with equal received interference power at SIR = 15dB. The desired signal and CCI signals are modulated by 4-QAM and 16-QAM, respectively.

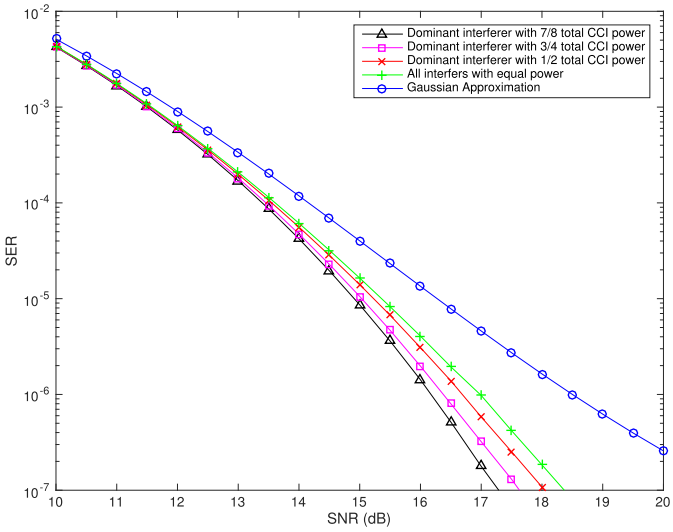

Fig. 4. SER versus SNR for 8 interferers at SIR = 15dB. The received interference power is dominated by one interferer, whereas other interferers have equal received power. The desired and CCI signals use 4-QAM and 16-QAM, respectively.

accuracy of the GA for the interference by comparing the resultant SER with the exact SER result.

Fig. 2 shows the SER versus SNR for the 4-QAM desired signal and a 16-QAM CCI signal, both using a raised cosine pulse with roll-off factor $\beta = 0.5$ at SIR= 10dB, 15dB and 20dB. The solid lines stand for the SERs obtained using the analytical expression (34) with $L = 20$, and the crosses denote the SERs obtained by Monte Carlo simulation. In the simulation, each data point is generated by averaging over 10^9 symbols. We observe that the analytical results are in excellent agreement with the simulation. Therefore, we show the results obtained by the analytical expression with $L = 20$ in the remaining examples. Although we only show 4-QAM for the desired signal and 16-QAM for the interference at several SIR values as examples in Fig. 2, we have simulated all combinations of alphabet sizes from 4-QAM, 16-QAM, 64-QAM and 256-QAM for the desired and interference signals, and at other SIR values, and the analytical results are all in good agreement with simulations.

Fig. 3 presents how SER changes as the number of interferers increases, given a fixed received SIR and letting the interference power be equally distributed among all received interference signals. We observe from Fig. 3 that the SER increases as the number of CCI signals increases, and the gap between the analytical SER result and the SER obtained by the GA becomes smaller, which is the consequence of the central limit theorem.

We also consider the interference dominated by one interferer. Fig. 4 presents the SER for 8 interferers as the received interference power becomes more dominated by a single interferer. As the power of the dominant interferer accounts for a larger proportion of the total received interference power, the exact SER becomes smaller. It is seen that the GA is more pessimistic in evaluating the SER when the received interference power is more dominated by a single interferer.

It is observed in Figures 2 - 4 that the GA overestimates the SER for QAM in CCI. The gap between the GA and the analytical SER expression is negligible at low SNR but is significant at high SNR. For example, when the SER target equals 10^{-3} and SIR=10dB, a SNR gap that is larger than 5dB is observed in Fig. 2 between the exact SER expression and the SER obtained by the GA. This behavior can be explained by the unbounded tail of Gaussian RVs. The QAM CCI signal at the output of the matched filter is bounded, if a pulse from the parametric family defined in (2) is used. However, the GA generates an unbounded tail for the CCI, which increases the estimated SER at high SNR.

B. Results of Resource Allocation for D2D Video Transmission

We simulate a D2D system with $M_c = 8$ subcarriers, each with bandwidth 15kHz. The roll-off factor for the raised-cosine pulse is $\beta = 0.5$, and the symbol rate is $1/T = 10$kHz. The channel response consists of path loss, shadowing and multipath fading. The path loss is $46.8 + 18.7 \log_{10}(d[m])$

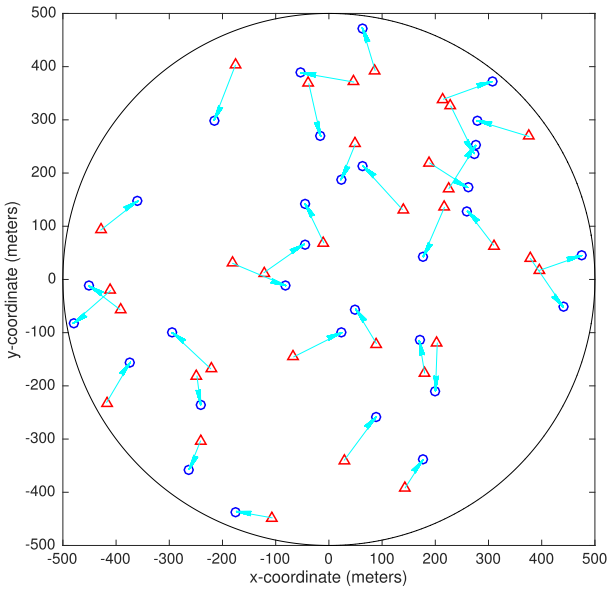

Fig. 5. Example of a cell with 32 D2D pairs.

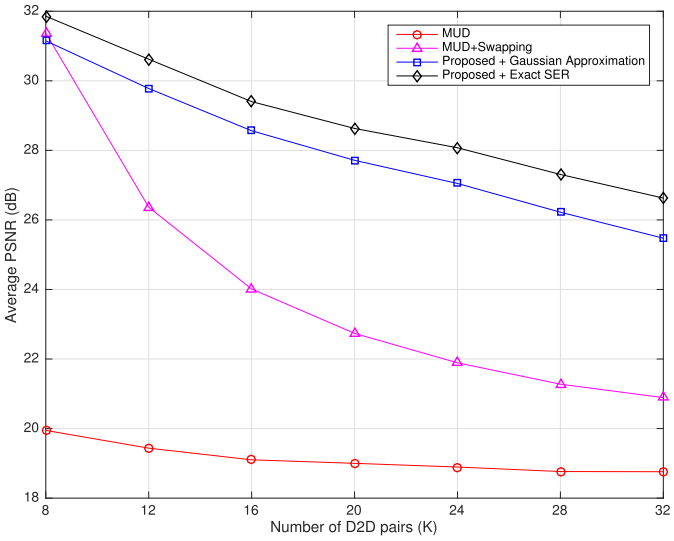

Fig. 6. Video PSNR versus the number of D2D pairs for the proposed algorithms using the GA or the exact SER, compared with baseline algorithms.

and the shadowing follows the log-normal distribution with standard deviation of 3dB [40]. The subcarriers experience independent Rayleigh fading due to multipath, and the channel response is assumed to be flat within a subcarrier. The maximal transmission power for each D2D pair is 100mW. The SER target is 10^{-3} in the simulation. The supported modulation formats are 4-QAM, 16-QAM and 64-QAM.

We generate 10^3 realizations of geographical locations in the simulation, each with independent channels. For each realization of geographical location, we first initialize an empty D2D pair list. We repeatedly generate a transmitter and a receiver that are each uniformly distributed in a cell of a radius of 500 meters. The D2D distance is set between 10 and 50 meters. If the distance between the newly generated pair is within this range of 10 to 50 meters, the newly generated pair is considered suitable for D2D transmission, and therefore it is added to the list. This procedure is repeated until the number of D2D pairs in the list reaches the desired number K. Fig. 5 shows a realization of the cell with $K = 32$ D2D pairs.

We use a video sequence with a resolution of 640×480, encoded using H.264/SVC reference software JSVM version 9.19.15. The total length of the video is 30 seconds at 30 frames per second, and the video is organized in GOPs of 15 frames (I-P-P-P). By assigning random starting points of the same cyclic video to different D2D pairs, we create application layer diversity among D2D pairs and yet have the same average complexity over time for different D2D pairs. The 4×4 DCT coefficients for the MGS layer of each macroblock are split with MGS vector $[1, 1, 2, 2, 2, 8]$ [34]. The video contents are protected by a rate $2/3$ punctured turbo code. Each packet consists of 300 bytes of FEC plus data bits. The video quality is evaluated by peak signal-to-noise ratio (PSNR), which is defined by $\text{PSNR} = 10 \log_{10} \frac{255^2}{\mathbb{E}[\text{MSE}]}$.

We simulate the performance of the proposed cross-layer algorithm combined with either the exact SER expression or the GA. In Fig. 6, the PSNR gap between the proposed SER expression and the GA is approximately 1dB. When the proposed resource allocation algorithm with the GA will admit 24 users with an average PSNR of approximately 27dB, the same algorithm with the proposed SER expression will be able to admit 30 users. Two baseline algorithms are also used for comparison. The first uses MUD, namely Step 1 of the proposed algorithm; the second baseline algorithm is the iterative orthogonal subcarrier assignment algorithm with subcarrier swapping from [26]. The proposed resource allocation algorithm outperforms the baseline algorithms by a PSNR gap that is larger than 5dB for 20 to 32 D2D pairs.

To explain the underlying reasons for the gap between the video PSNR using the exact SER and the GA for resource allocation, the distribution of the number of D2D pairs in a subcarrier is presented in Fig. 7. More than 95% of subcarriers simulated are assigned to between 2 and 6 D2D pairs. This simulation result indicates that the number of D2D pairs sharing a subcarrier is typically small, even if the number of D2D pairs in the system is much larger than the number of subcarriers, which is one reason that the GA is not applicable for this scenario.

The other reason that undermines the accuracy of the GA is that it is highly possible that the received interference power is dominated by a single interferer. Fig. 8 shows the cumulative distribution of the power ratio of the dominant interferer over the total interference power at D2D receivers. The cumulative distribution is calculated at each D2D receiver for the cases that at least 4 D2D pairs are allocated in a subcarrier, using the proposed algorithm with the exact SER. As K ranges from 8 to 32, the probability of the dominant interferer accounting for more than half of the total received interference power is larger than 0.75. For the case of 8 D2D pairs in the cell, there is a probability of 0.5 that the dominant interferer takes larger than $3/4$ of the total received interference power.

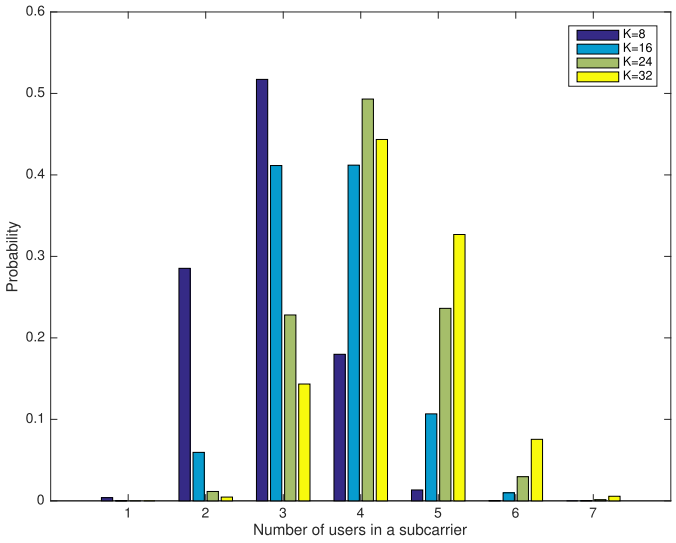

Fig. 7. The distribution of the number of D2D pairs assigned to a subcarrier, by the proposed algorithm using the exact SER.

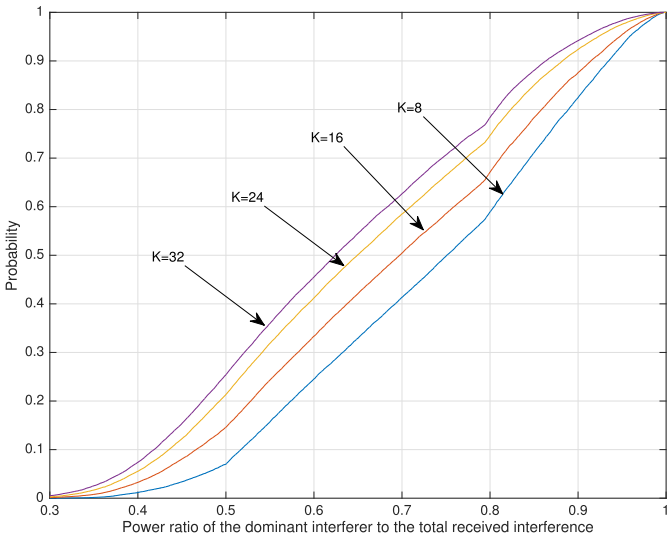

Fig. 8. The cumulative distribution of the power ratio of the dominant interferer to the total interference at D2D receivers given that there are at least 4 D2D pairs in a subcarrier.

VI. Conclusion

This paper makes two main contributions: (1) We derived an analytical and exact SER expression for D2D systems using multicarrier bandlimited QAM signaling, and (2) we developed a novel resource allocation algorithm for multicarrier D2D video transmission. The new algorithm outperforms MUD resource allocation as well as a previous method in the literature when using the conventional method of SER evaluation involving approximating the interference as Gaussian. Further gains were demonstrated from using the newly derived SER expression in the resource allocation algorithm. The small number of interferers in the multicarrier D2D system and the high probability of a dominant interferer both undermine the accuracy of the GA.

Appendix A
Proof of Proposition 1

Define RVs $Y_i^I \triangleq \sqrt{P_i T}\sum_{s=-\infty}^{\infty} X_i^I[s]\, g(-\tau_i - sT)$, $Y_i^Q \triangleq \sqrt{P_i T}\sum_{s=-\infty}^{\infty} X_i^Q[s]\, g(-\tau_i - sT)$, where $X_i^I[s] \triangleq \mathrm{Re}(X_i[s])$ and $X_i^Q[s] \triangleq \mathrm{Im}(X_i[s])$ are the in-phase and quadrature components of the s-th symbol in the i-th transmitted QAM signal. Given τ_i, the conditional CF of Y_i^I is

$$\begin{aligned}
&\varphi_{Y_i^I|\tau_i}(u|\tau_i)\\
&= \prod_{s=-\infty}^{\infty} E\left[e^{ju\sqrt{P_i T}X_i^I[s]g(-\tau_i - sT)}\middle|\tau_i\right]\\
&= \prod_{s=-\infty}^{\infty} \frac{1}{\sqrt{M_{i,m}}} \sum_{n=-(\sqrt{M_{i,m}}/2-1)}^{\sqrt{M_{i,m}}/2} e^{ju(2n-1)g(-\tau_i - sT)A_i}\\
&= \prod_{s=-\infty}^{\infty} \frac{2}{\sqrt{M_{i,m}}} \sum_{n=1}^{\sqrt{M_{i,m}}/2} \cos\Big(u(2n-1)g(-\tau_i - sT)A_i\Big),
\end{aligned} \tag{A.1}$$

where A_i is given by (13). Let $I_i^I = \mathrm{Re}(I_i)$ and $I_i^Q = \mathrm{Im}(I_i)$. From (8), I_i^I are given by

$$\begin{aligned}
I_i^I &= \sqrt{P_i T}\sum_{s=-\infty}^{\infty} (X_i^I[s]\cos\phi_i - X_i^Q[s]\sin\phi_i) g(-\tau_i - sT)\\
&= Y_i^I\cos\phi_i - Y_i^Q\sin\phi_i.
\end{aligned} \tag{A.2}$$

Similarly, we obtain that $I_i^Q = Y_i^I\sin\phi_i + Y_i^Q\cos\phi_i$ and $\varphi_{Y_i^Q|\tau_i}(u|\tau_i)$ is identical to $\varphi_{Y_i^Q|\tau_i}(u|\tau_i)$ in (A.1).

Since $X_i^I[s_1]$ and $X_i^Q[s_2]$ are independent, Y_i^I and Y_i^Q are conditionally independent, given τ_i. Given ϕ_i and τ_i, the conditional joint CF of I_i^I and I_i^Q is given by

$$\begin{aligned}
&\varphi_{I_i^I, I_i^Q|\tau_i,\phi_i}(u, v|\tau_i, \phi_i)\\
&= E\left[e^{j(uI_i^I + vI_i^Q)}\middle|\tau_i, \phi_i\right]\\
&= E\left[e^{jY_i^I(u\cos\phi_i + v\sin\phi_i) + jY_i^Q(v\cos\phi_i - u\sin\phi_i)}\middle|\tau_i, \phi_i\right]\\
&= E\left[e^{jY_i^I(u\cos\phi_i + v\sin\phi_i)}\middle|\tau_i, \phi_i\right]\cdot E\left[e^{jY_i^Q(v\cos\phi_i - u\sin\phi_i)}\middle|\tau_i, \phi_i\right]\\
&= \varphi_{Y_i^I|\tau_i}\Big(u\cos\phi_i + v\sin\phi_i\Big|\tau_i\Big)\cdot\varphi_{Y_i^Q|\tau_i}\Big(v\cos\phi_i - u\sin\phi_i\Big|\tau_i\Big).
\end{aligned} \tag{A.3}$$

Substituting (A.1) and $\varphi_{Y_i^Q|\tau_i}(u|\tau_i) = \varphi_{Y_i^I|\tau_i}(u|\tau_i)$ into (A.3) finishes the proof.

Appendix B
Proof of Proposition 2

The aim of this section is to expand the joint CF of I^I and I^Q ($\varphi_{I^I,I^Q}(u,v)$) into a power series. To proceed, the following lemma is useful:

Lemma 1: Consider power series $a(y) = \sum_{n=0}^{\infty} a_n y^n$ and $c(y) = \ln[a(y)]$. The power series expansion of $c(y)$ is denoted by $c(y) = \sum_{n=0}^{\infty} c_n y^n$. If $a_0 = 1$, then a recursive

relation for the $\{c_n\}$ is given by $c_0 = 0$ and

$$c_n = a_n - \sum_{p=1}^{n-1} \frac{p}{n} c_p a_{n-p}, \tag{B.1}$$

for positive n. Conversely, if $c_0 = 0$, then $a_0 = 1$ and the following recursive relation for the $\{a_n\}$ holds for positive n:

$$a_n = \sum_{p=1}^{n} \frac{p}{n} c_p a_{n-p}. \tag{B.2}$$

Proof: The proof is by differentiation and Leibniz's rule [39, 0.42] and is omitted here because of page limitations. ∎

We denote $g_s(\tau_i) = g(-\tau_i - sT)$, $\rho = (u^2 + v^2)^{1/2}$ and $\theta = \tan^{-1}(v/u)$. Therefore, $u = \rho\cos\theta$ and $v = \rho\sin\theta$. From Theorem 1, the conditional joint CF of I_i^I and I_i^Q, given ϕ_i and τ_i, can be written as

$$\begin{aligned}
&\varphi_{I_i^I, I_i^Q|\tau_i,\phi_i}(u, v|\tau_i, \phi_i) \\
&= \prod_{s_1=-\infty}^{\infty} \frac{2}{\sqrt{M_{i,m}}} \sum_{j=1}^{\sqrt{M_{i,m}}/2} \\
&\quad \times \cos\Big(A_i\rho\cos(\theta - \phi_i)(2j-1)g_{s_1}(\tau_i)\Big) \\
&\quad \cdot \prod_{s_2=-\infty}^{\infty} \frac{2}{\sqrt{M_{i,m}}} \sum_{l=1}^{\sqrt{M_{i,m}}/2} \\
&\quad \times \cos\Big(A_i\rho\sin(\theta - \phi_i)(2l-1)g_{s_2}(\tau_i)\Big).
\end{aligned}$$

To proceed, we define the following two auxiliary functions:

$$f^{(M)}(x, \tau, s) = \frac{2}{\sqrt{M}} \sum_{j=1}^{\sqrt{M}/2} \cos\Big(x(2j-1)g_s(\tau)\Big), \tag{B.3}$$

$$\Phi^{(M)}(x, \tau) = \sum_{s=-\infty}^{\infty} \ln\Big[f^{(M)}(x, \tau, s)\Big]. \tag{B.4}$$

Therefore, the conditional joint CF satisfies

$$\begin{aligned}
&\varphi_{I_i^I, I_i^Q|\tau_i,\phi_i}(u, v|\tau_i, \phi_i) \\
&= \prod_{s_1=-\infty}^{\infty} f^{(M_{i,m})}(A_i\rho\cos(\theta - \phi_i), \tau_i, s_1) \\
&\quad \cdot \prod_{s_2=-\infty}^{\infty} f^{(M_{i,m})}(A_i\rho\sin(\theta - \phi_i), \tau_i, s_2) \\
&= \exp\Big[\Phi^{(M_{i,m})}(A_i\rho\cos(\theta - \phi_i), \tau_i)\Big] \\
&\quad \cdot \exp\Big[\Phi^{(M_{i,m})}(A_i\rho\sin(\theta - \phi_i), \tau_i)\Big].
\end{aligned} \tag{B.5}$$

Using the power series $\cos(y) = \sum_{n=0}^{\infty} \frac{(-1)^n}{(2n)!} y^{2n}$ from [39, 1.411 (3)] in (B.3), we obtain

$$\begin{aligned}
&f^{(M)}(x, \tau, s) \\
&= \frac{2}{\sqrt{M}} \sum_{i=1}^{\sqrt{M}/2} \sum_{n=0}^{\infty} \frac{(-1)^n}{(2n)!} \Big(x(2i-1)g_s(\tau)\Big)^{2n} \\
&= \sum_{n=0}^{\infty} \left[\frac{1}{(2n)!} \frac{2}{\sqrt{M}} \sum_{l=1}^{\sqrt{M}/2} (2l-1)^{2n}\right] (-1)^n g_s^{2n}(\tau) x^{2n}.
\end{aligned} \tag{B.6}$$

Let $a_n^{(M)} \triangleq 2/[(2n)!\sqrt{M}] \sum_{l=1}^{\sqrt{M}/2} (2l-1)^{2n}$, so that $f^{(M)}(x, \tau, s) = \sum_{n=0}^{\infty} a_n^{(M)} (-1)^n g_s^{2n}(\tau) x^{2n}$. It can be verified that $a_0^{(M)} = 1$. Invoking Lemma 1 in (B.6), we have

$$\ln[f^{(M)}(x, \tau, s)] = \sum_{n=0}^{\infty} c_n^{(M)} (-1)^n g_s^{2n}(\tau) x^{2n}, \tag{B.7}$$

where $c_0^{(M)} = 0$ and the following recursive relation holds for positive integer n:

$$c_n^{(M)} = a_n^{(M)} - \sum_{p=1}^{n-1} \frac{p}{n} c_p^{(M)} a_{n-p}^{(M)}. \tag{B.8}$$

Substituting (B.7) into (B.4) yields

$$\begin{aligned}
\Phi^{(M)}(x, \tau) &= \sum_{s=-\infty}^{\infty} \sum_{n=0}^{\infty} c_n^{(M)} (-1)^n g_s^{2n}(\tau) x^{2n} \\
&= \sum_{n=0}^{\infty} \left[c_n^{(M)} \sum_{s=-\infty}^{\infty} g_s^{2n}(\tau)\right] (-1)^n x^{2n}.
\end{aligned} \tag{B.9}$$

Invoking Lemma 1 in (B.9), we obtain

$$\exp\big[\Phi^{(M)}(x, \tau)\big] = \sum_{n=0}^{\infty} \zeta_n^{(M)}(\tau) (-1)^n x^{2n}, \tag{B.10}$$

where $\zeta_0^{(M)}(\tau) = 1$ and the following recursive relation holds for positive integer n:

$$\zeta_n^{(M)}(\tau) = \sum_{p=1}^{n} \frac{p}{n} \Big[c_p^{(M)} \sum_{s=-\infty}^{\infty} g_s^{2p}(\tau)\Big] \zeta_{n-p}^{(M)}(\tau). \tag{B.11}$$

Because (B.11) is a recursive expression, we cannot directly compute the average of $\zeta_n^{(M)}(\tau)$ over τ. We use a method inspired by [8, eq. (45)] to write $\zeta_n^{(M)}(\tau)$ as a function of two components: one is only dependent on M and $g(t)$, and the other one is only dependent on τ. Recall that $g(t)$ is a Nyquist pulse, and let $G_m(f)$ be the Fourier transform of $[g(t)]^m$, $m \geq 1$, given by $G_m(f) = \int_{-\infty}^{\infty} [g(t)]^m e^{-j2\pi ft}\, dt$. Regarding $G_m(f)$, we have the following lemma:

Lemma 2: $G_m(f) = 0$ for $|f| > m/T$, where $m \geq 1$.

Proof: Note that $G_1(f) = G(f)$ is zero for $|f| > 1/T$ according to (2). Assume that $G_{m_0-1}(f) = 0$ for $|f| > (m_0 - 1)/T$. Since $G_{m_0}(f) = G_{m_0-1}(f) * G_1(f)$, where $*$ stands for convolution, we know $G_{m_0}(f) = 0$ for $|f| > (m_0 - 1)/T + 1/T = m_0/T$. By induction this lemma is proved. ∎

From the well-known Poisson summation formula [36, p. 47, (3-56)], $\sum_{s=-\infty}^{\infty} g_s^{2n}(\tau) = \sum_{s=-\infty}^{\infty}[g(-sT-\tau)]^{2n} = (1/T)\sum_{s=-\infty}^{\infty} G_{2n}(s/T)\exp(j2\pi\tau s/T)$. Since $g^{2n}(t)$ is real-valued, $G_{2n}(-f) = G_{2n}^*(f)$. Therefore, $\sum_{s=-\infty}^{\infty} g_s^{2n}(\tau)$ is further given by

$$\sum_{s=-\infty}^{\infty} g_s^{2n}(\tau) = \sum_{s=0}^{\infty} \frac{2-\delta_s}{T}\mathrm{Re}\left[G_{2n}\left(\frac{s}{T}\right)\exp\left(j\frac{2\pi\tau s}{T}\right)\right], \tag{B.12}$$

where δ_s is the Kronecker delta function. Invoking Lemma 2, (B.12) reduces to

$$\sum_{s=-\infty}^{\infty} g_s^{2n}(\tau) = \sum_{s=0}^{2n} \frac{2-\delta_s}{T}\left\{\mathrm{Re}\left[G_{2n}\left(\frac{s}{T}\right)\right]\cos\left(\frac{2\pi\tau s}{T}\right) - \mathrm{Im}\left[G_{2n}\left(\frac{s}{T}\right)\right]\sin\left(\frac{2\pi\tau s}{T}\right)\right\}. \tag{B.13}$$

We obtain $\sin sx = \sum_{l=0,\, l\ \text{odd}}^{s}\binom{s}{l}(-1)^{(l-1)/2}\cos^{s-l}x\sin^l x$ and $\cos sx = \sum_{l=0,\, l\ \text{even}}^{s}\binom{s}{l}(-1)^{l/2}\cos^{s-l}x\sin^l x$ from [39, 1.331 (1),(3)], hence (B.13) yields

$$\sum_{s=-\infty}^{\infty} g_s^{2n}(\tau) = \sum_{s=0}^{2n}\sum_{s_1=0}^{s}\cos^{s-s_1}\left(\frac{2\pi\tau}{T}\right)\sin^{s_1}\left(\frac{2\pi\tau}{T}\right)R_n(s,s_1), \tag{B.14}$$

where $R_n(s,s_1)$ is given by (22). By comparing (B.11) and (B.14), $\zeta_n^{(M)}(\tau)$ can be put into the following form:

$$\zeta_n^{(M)}(\tau) = \sum_{s=0}^{2n}\sum_{s_1=0}^{s}\cos^{s-s_1}\left(\frac{2\pi\tau}{T}\right)\sin^{s_1}\left(\frac{2\pi\tau}{T}\right)w_n^{(M)}(s,s_1), \tag{B.15}$$

where $\{w_n^{(M)}(s,s_1)\}$ is a set of coefficients defined for $0 \le s_1 \le s \le 2n$ whose recursion is to be determined. For $n \ge 1$, substituting (B.15) and (B.14) into the righthand side of (B.11), we have

$$\begin{aligned}
&\zeta_n^{(M)}(\tau)\\
&= \sum_{p=1}^{n}\frac{p}{n}c_p^{(M)}\Big[\sum_{s=-\infty}^{\infty} g_s^{2p}(\tau)\Big]\zeta_{n-p}^{(M)}(\tau)\\
&= \sum_{p=1}^{n}\frac{p}{n}c_p^{(M)}\Big[\sum_{s=0}^{2p}\sum_{s_1=0}^{s}\cos^{s-s_1}\Big(\frac{2\pi\tau}{T}\Big)\sin^{s_1}\Big(\frac{2\pi\tau}{T}\Big)R_p(s,s_1)\Big]\\
&\quad\cdot\Big[\sum_{s_2=0}^{2(n-p)}\sum_{s_3=0}^{s_2}\cos^{s_2-s_3}\left(\frac{2\pi\tau}{T}\right)\sin^{s_3}\left(\frac{2\pi\tau}{T}\right)w_{n-p}^{(M)}(s_2,s_3)\Big].
\end{aligned} \tag{B.16}$$

Substituting $s+s_2$ with q, s_1+s_3 with q_1, s with q_2, and s_1 with q_3 in (B.16), and after some manipulations, we obtain

$$\begin{aligned}
&\zeta_n^{(M)}(\tau)\\
&= \sum_{q=0}^{2n}\sum_{q_1=0}^{q}\cos^{q-q_1}\left(\frac{2\pi\tau}{T}\right)\sin^{q_1}\left(\frac{2\pi\tau}{T}\right)\sum_{p=1}^{n}\frac{p}{n}c_p^{(M)}\\
&\quad\cdot\sum_{q_2=\max(0,q+2p-2n)}^{\min(q,2p)}\ \sum_{q_3=\max(0,q_1+q_2-q)}^{\min(q_1,q_2)}\\
&\quad\times R_p(q_2,q_3)w_{n-p}^{(M)}(q-q_2,q_1-q_3).
\end{aligned} \tag{B.17}$$

Comparing (B.15) and (B.17), for $n \ge 1$, $0 \le q_1 \le q \le 2n$, we have

$$\begin{aligned}
w_n^{(M)}(q,q_1) &= \sum_{p=1}^{n}\frac{p}{n}c_p^{(M)}\sum_{q_2=\max(0,q+2p-2n)}^{\min(q,2p)}\ \sum_{q_3=\max(0,q_1+q_2-q)}^{\min(q_1,q_2)}R_p(q_2,q_3)\\
&\quad\cdot w_{n-p}^{(M)}(q-q_2,q_1-q_3).
\end{aligned} \tag{B.18}$$

Substituting $n = 0$ and $\zeta_0^{(M)}(\tau) = 1$ into (B.15), we obtain $w_0^{(M)}(0,0) = 1$. Therefore, the recursive relation of $\{w_n^{(M)}(q,q_1)\}$ is given by $w_0^{(M)}(0,0) = 1$ and (B.18).

Also, substituting (B.10) into (B.5) yields

$$\begin{aligned}
&\varphi_{I_i^I,I_i^Q|\tau_i,\phi_i}(u,v|\tau_i,\phi_i)\\
&= \sum_{p=0}^{\infty}\zeta_p^{(M)}(\tau_i)\cos^{2p}(\theta-\phi_i)(-A_i^2\rho^2)^p\\
&\quad\cdot\sum_{m=0}^{\infty}\zeta_m^{(M)}(\tau_i)\sin^{2m}(\theta-\phi_i)(-A_i^2\rho^2)^m.
\end{aligned} \tag{B.19}$$

Using the Cauchy product [41, p. 10] of two power series, $\varphi_{I_i^I,I_i^Q|\tau_i,\phi_i}(u,v|\tau_i,\phi_i)$ can be further written as

$$\varphi_{I_i^I,I_i^Q|\tau_i,\phi_i}(u,v|\tau_i,\phi_i) = \sum_{n=0}^{\infty}\xi_n^{(M_{i,m})}(u,v,\tau_i,\phi_i)(-A_i^2\rho^2)^n, \tag{B.20}$$

where $\xi_n^{(M_{i,m})}(u,v,\tau_i,\phi_i)$ is given by

$$\begin{aligned}
\xi_n^{(M_{i,m})}(u,v,\tau_i,\phi_i) &= \sum_{p=0}^{n}\zeta_p^{(M_{i,m})}(\tau_i)\zeta_{n-p}^{(M_{i,m})}(\tau_i)\cos^{2p}(\theta-\phi_i)\\
&\quad\cdot\sin^{2(n-p)}(\theta-\phi_i).
\end{aligned} \tag{B.21}$$

Substituting (B.15) into (B.21) yields

$$\begin{aligned}
&\xi_n^{(M_{i,m})}(u,v,\tau_i,\phi_i)\\
&= \sum_{p=0}^{n}\cos^{2p}(\theta-\phi_i)\sin^{2(n-p)}(\theta-\phi_i)\\
&\quad\cdot\sum_{s=0}^{2p}\sum_{s_1=0}^{s}\cos^{s-s_1}\left(\frac{2\pi\tau_i}{T}\right)\sin^{s_1}\left(\frac{2\pi\tau_i}{T}\right)w_p^{(M_{i,m})}(s,s_1)\\
&\quad\cdot\sum_{s_2=0}^{2(n-p)}\sum_{s_3=0}^{s_2}\cos^{s_2-s_3}\left(\frac{2\pi\tau_i}{T}\right)\sin^{s_3}\left(\frac{2\pi\tau_i}{T}\right)w_{n-p}^{(M_{i,m})}(s_2,s_3).
\end{aligned}$$

Substituting $s+s_2$ with q, s_1+s_3 with q_1, s with q_2 and s_1 with q_3 yields

$$\begin{aligned}&\xi_n^{(M_{i,m})}(u,v,\tau_i,\phi_i)\\&=\sum_{p=0}^{n}\cos^{2p}(\theta-\phi_i)\sin^{2(n-p)}(\theta-\phi_i)\\&\quad\cdot\sum_{q=0}^{2n}\sum_{q_1=0}^{q}\cos^{t-q_1}\left(\frac{2\pi\tau_i}{T}\right)\sin^{q_1}\left(\frac{2\pi\tau_i}{T}\right)\sum_{q_2=\max(0,q+2p-2n)}^{\min(q,2p)}\\&\quad\cdot\sum_{q_3=\max(0,q_1+q_2-q)}^{\min(q_1,q_2)}w_p^{(M_{i,m})}(q_2,q_3)\,w_{n-p}^{(M_{i,m})}(q-q_2,q_1-q_3).\end{aligned}\tag{B.22}$$

Notice that $2\pi\tau_i/T$ and ϕ_i are both uniformly distributed in $[0,2\pi)$. We define $B_{m,n}\triangleq\frac{1}{2\pi}\int_0^{2\pi}\cos^m\phi\sin^n\phi\,d\phi$, whose value is given by [39, 3.621 (5)]

$$B_{m,n}=\begin{cases}\frac{(m-1)!!(n-1)!!}{(m+n)!!}, & m,n\geq 0,\ m,n\text{ even},\\0, & \text{otherwise.}\end{cases}\tag{B.23}$$

Using $\{B_{m,n}\}$, the expectation of $\xi_n^{(M_{i,m})}(u,v,\tau_i,\phi_i)$ in (B.22) is given by

$$\begin{aligned}&E_{\tau_i,\phi_i}[\xi_n^{(M_{i,m})}(u,v,\tau_i,\phi_i)]\\&=\sum_{p=0}^{n}B_{2p,2(n-p)}\sum_{t=0}^{2n}\sum_{q_1=0}^{q}B_{q_1,q-q_1}\sum_{q_2=\max(0,q+2p-2n)}^{\min(q,2p)}\\&\quad\cdot\sum_{q_3=\max(0,q_1+q_2-q)}^{\min(q_1,q_2)}w_p^{(M_{i,m})}(q_2,q_3)w_{n-p}^{(M_{i,m})}(q-q_2,q_1-q_3).\end{aligned}\tag{B.24}$$

From (B.20), we can express the joint CF of I_i^I and I_i^Q as

$$\begin{aligned}\varphi_{I_i^I,I_i^Q}(u,v)&=E_{\tau_i,\phi_i}[\varphi_{I_i^I,I_i^Q|\tau_i,\phi_i}(u,v|\tau_i,\phi_i)]\\&=\sum_{n=0}^{\infty}E_{\tau_i,\phi_i}[\xi_n^{(M_{i,m})}(u,v,\tau_i,\phi_i)](-A_i^2\rho^2)^n.\end{aligned}\tag{B.25}$$

Using (13), (B.24) and $\rho=\sqrt{u^2+v^2}$ in (B.25) yields

$$\begin{aligned}&\varphi_{I_i^I,I_i^Q}(u,v)\\&\quad=\sum_{n=0}^{\infty}\Bigg[\sum_{p=0}^{n}B_{2p,2(n-p)}\sum_{q=0}^{2n}\sum_{q_1=0}^{q}B_{q_1,t-q_1}\sum_{q_2=\max(0,q+2p-2n)}^{\min(q,2p)}\\&\qquad\cdot\sum_{q_3=\max(0,q_1+q_2-t)}^{\min(q_1,q_2)}w_p^{(M_{i,m})}(q_2,q_3)w_{n-p}^{(M_{i,m})}(t-q_2,q_1-q_3)\Bigg]\\&\qquad\cdot\left[-\frac{3P_iT}{M_{i,m}-1}(u^2+v^2)\right]^n,\end{aligned}\tag{B.26}$$

Invoking Lemma 1 in (B.26), we obtain

$$\ln\left[\varphi_{I_i^I,I_i^Q}(u,v)\right]=\sum_{n=0}^{\infty}d_n^{(M_{i,m})}[-P_iT(u^2+v^2)]^n,\tag{B.27}$$

where the recursive relations of coefficients $\{d_n^{(M_{i,m})}\}$ are given by invoking Lemma 1 in (B.27) and (B.26).

Substituting (B.27) into (16), $\varphi_{I^I,I^Q}(u,v)$ is given by

$$\begin{aligned}&\varphi_{I^I,I^Q}(u,v)\\&=\exp\left[\sum_{i=1,i\neq k}^{K}\ln\left(\varphi_{I_i^I,I_i^Q}(u,v)\right)\right]\\&=\exp\left\{\sum_{n=0}^{\infty}\left[\sum_{i=1,i\neq k}^{K}(-P_iT)^nd_n^{(M_{i,m})}\right](u^2+v^2)^n\right\}\\&=\exp\left\{\sum_{n=0}^{\infty}\left[\sum_{i=1,i\neq k}^{K}\left(\frac{P_iT}{N_0}\right)^nd_n^{(M_{i,m})}\right](-N_0)^n(u^2+v^2)^n\right\}.\end{aligned}$$

Applying Lemma 1 to the last equality finishes the proof.

Appendix C
Convergence Analysis for SER Expression

We derive an upper bound for the magnitude of the truncation error for the proposed SER expression in (34). Suppose we use the terms with less than $2L$-th order in the power series expansion of the total CCI's CF for SER calculation. According to the Taylor theorem in multivariate functions [42, p. 360, Th. 13.3], the magnitude of error incurred by truncation is given by

$$\begin{aligned}&\left|\varphi_{I^I,I^Q}(u,v)-\sum_{n=0}^{L-1}b_n^{(k,m)}(-N_0)^n(u^2+v^2)^n\right|\\&\quad\leq\frac{(u^2+v^2)^L}{(2L)!}\max_{\substack{l=0,1,\cdots,2L\\0\leq u_0^2+v_0^2\leq u^2+v^2}}\left|\frac{\partial^{2L}}{\partial u_0^l\partial v_0^{2L-l}}\varphi_{I^I,I^Q}(u_0,v_0)\right|.\end{aligned}\tag{C.1}$$

The joint pdf of I^I and I^Q is denoted by $p_{I^I,I^Q}(x,y)$. Since $p_{I^I,I^Q}(x,y)$ is the Fourier transform of $\varphi_{I^I,I^Q}(u_0,v_0)$, it is well known that $(jx)^l(jy)^{2L-l}p_{I^I,I^Q}(x,y)$ is the Fourier transform of $\partial^{2L}/[\partial u_0^l\partial v_0^{2L-l}]\varphi_{I^I,I^Q}(u_0,v_0)$ [36, p. 16, eq. (2-41)]. Making use of this Fourier transform pair, we have

$$\begin{aligned}&\left|\frac{\partial^{2L}}{\partial u_0^l\partial v_0^{2L-l}}\varphi_{I^I,I^Q}(u_0,v_0)\right|\\&=\left|\int_{-\infty}^{\infty}\int_{-\infty}^{\infty}e^{j(u_0x+v_0y)}\Big[(jx)^l(jy)^{2L-l}p_{I^I,I^Q}(x,y)\Big]dxdy\right|\\&\leq\int_{-\infty}^{\infty}\int_{-\infty}^{\infty}|x|^l|y|^{2L-l}p_{I^I,I^Q}(x,y)dxdy\\&=E\left[|I^I|^l\,|I^Q|^{2L-l}\right]\leq E\Big[|I|^{2L}\Big],\end{aligned}\tag{C.2}$$

where the last inequality follows from $|I^I|=|\mathrm{Re}(I)|\leq|I|$ and $|I^Q|=|\mathrm{Im}(I)|\leq|I|$. Recall that, in (8), the aggregated CCI is given by $I=\sum_{i=1,i\neq k}^{K}\sqrt{P_iT}\sum_{s=-\infty}^{\infty}X_i[s]g(-\tau_i-sT)$, and the magnitude of the received QAM symbol is bounded using (13) by $\sqrt{P_iT}|X_i[s]|\leq\sqrt{2}(\sqrt{M_{i,m}}-1)A_i=\sqrt{2}(\sqrt{M_{i,m}}-1)[3P_iT/(M_{i,m}-1)]^{1/2}\leq\sqrt{6P_iT}$, so the magnitude of the aggregated CCI is bounded by

$$\begin{aligned}|I|&\leq\sum_{i=1,i\neq k}^{K}\max_{s'}(\sqrt{P_iT}|X_i[s']|)\sum_{s=-\infty}^{\infty}|g(-\tau_i-sT)|\\&\leq\sum_{i=1,i\neq k}^{K}\sqrt{6P_iT}\cdot C,\end{aligned}\tag{C.3}$$

where the maximum inter-symbol interference for the Nyquist pulse is defined as $C \triangleq \sup_{0<\tau<T}\{\sum_{s=-\infty}^{\infty}|g(\tau-sT)|\}$. Using the results in [30], C is shown to be a finite constant for the family of Nyquist pulses that are defined in (2). A special case of C is given by Proposition 3.

Proposition 3: For a raised-cosine pulse with roll-off factor $\beta = 0.5$, $C = 10\sqrt{2}/(3\pi)$.

Proof: The raised-cosine pulse is given by $g(t) = \text{sinc}\,(\pi t/T)\cdot\cos(\pi\beta t/T)/(1-4\beta^2t^2/T^2)$ from [30]. For $\beta = 0.5$, $g(-\tau - sT) = g[(a+s)T] = \{\sin(\pi a)/[\pi(a+s)]\}\cdot\{\cos[(\pi/2)(a+s)]/[1-(a+s)^2]\}$, where $a = \tau/T$ and $0 < a < 1$. Letting $\psi(a,p) \triangleq 1/\{(a+p)[(a+p)^2-1]\}$, we have

$$\sum_{s=-\infty}^{\infty}|g((a+s)T)| = \frac{\sin(\pi a)}{\pi}\Bigg[\cos\left(\frac{\pi}{2}a\right)\sum_{n=-\infty}^{\infty}|\psi(a,2n)| + \sin\left(\frac{\pi}{2}a\right)\sum_{l=-\infty}^{\infty}|\psi(a,2l+1)|\Bigg]. \tag{C.4}$$

Notice that $\psi(a,p) = 1/[2(a+p-1)] - 1/(a+p) + 1/[2(a+p+1)]$. For $n \geq 1$, $\psi(a,2n) > 0$ and $\psi(a,2n) < 0$ otherwise. For $l \geq -1$, $\psi(a,2l+1) > 0$ and $\psi(a,2l+1) < 0$ otherwise. Therefore, (C.4) reduces to

$$\sum_{s=-\infty}^{\infty}|g((a+s)T)| = \frac{\sin(\pi a)}{\pi}\Bigg[\cos\left(\frac{\pi}{2}a\right)\left(\sum_{n_1=0}^{\infty}\frac{(-1)^{n_1}}{a-n_1} - \sum_{n_2=2}^{\infty}\frac{(-1)^{n_2}}{a+n_2}\right) + \sin\left(\frac{\pi}{2}a\right)\left(\sum_{l_1=-1}^{\infty}\frac{(-1)^{l_1}}{a+l_1} - \sum_{l_2=3}^{\infty}\frac{(-1)^{l_2}}{a-l_2}\right)\Bigg]. \tag{C.5}$$

We can verify that the maximum of (C.5) is achieved at $a = 1/2$. Substituting $a = 1/2$, (C.5) yields

$$C = \frac{1}{\pi}\left[\frac{\sqrt{2}}{2}\sum_{n=0}^{2}\frac{(-1)^n}{\frac{1}{2}-n} + \frac{\sqrt{2}}{2}\sum_{l=-1}^{1}\frac{(-1)^l}{\frac{1}{2}+l}\right] = \frac{10\sqrt{2}}{3\pi}. \tag{C.6}$$

■

We further substitute (C.2) and (C.3) into (C.1) to obtain

$$\left|\varphi_{I^I,I^Q}(u,v) - \sum_{n=0}^{L-1}b_n^{(k,m)}(-N_0)^n(u^2+v^2)^n\right| \leq \frac{(u^2+v^2)^L}{(2L)!}\left(C\sum_{i=1,i\neq k}^{K}\sqrt{6P_iT}\right)^{2L}. \tag{C.7}$$

Let $\Pr(\mathcal{B}_1;2L)$ be the truncated expression obtained by retaining the terms with order less than $2L$ in the expression $\Pr(\mathcal{B}_1)$ in (31). The truncation error is bounded by

$$\begin{aligned}
&\left|\Pr(\mathcal{B}_1) - \Pr(\mathcal{B}_1;2L)\right| \\
&= \left|\frac{1}{\pi^2}\int_{-\infty}^{\infty}\int_{-\infty}^{\infty}\frac{\sin(A_ku)}{u}\frac{\sin(A_kv)}{v}e^{-\frac{(u^2+v^2)N_0}{2}} \cdot\left[\varphi_{I^I,I^Q}(u,v) - \sum_{n=0}^{L-1}b_n^{(k,m)}(-N_0)^n(u^2+v^2)^n\right]dudv\right| \\
&< \frac{A_k^2}{\pi^2}\int_{-\infty}^{\infty}\int_{-\infty}^{\infty}\left|\varphi_{I^I,I^Q}(u,v) - \sum_{n=0}^{L-1}b_n^{(k,m)}(-N_0)^n(u^2+v^2)^n\right| \cdot e^{-\frac{(u^2+v^2)N_0}{2}}dudv \\
&\leq \frac{A_k^2}{\pi^2(2L)!}\left(C\sum_{i=1,i\neq k}^{K}\sqrt{6P_iT}\right)^{2L} \cdot\int_{-\infty}^{\infty}\int_{-\infty}^{\infty}(u^2+v^2)^Le^{-\frac{(u^2+v^2)N_0}{2}}dudv,
\end{aligned} \tag{C.8}$$

which follows from $|\sin(ax)/x| \leq |a|$ and (C.7). By substituting u with $\sqrt{r}\cos\varphi$ and v with $\sqrt{r}\sin\varphi$, we have $\int_{-\infty}^{\infty}\int_{-\infty}^{\infty}(u^2+v^2)^L\exp[-(u^2+v^2)N_0/2]dudv = \int_0^{2\pi}\int_0^{\infty}r^L\exp(-rN_0/2)(1/2)drd\varphi = \pi L!/(N_0/2)^{L+1}$, where the last equality is from [39, 3.381(4)]. Then (C.8) reduces to

$$|\Pr(\mathcal{B}_1) - \Pr(\mathcal{B}_1;2L)| < \frac{2A_k^2}{\pi N_0}\left(C\sum_{i=1,i\neq k}^{K}\sqrt{\frac{6P_iT}{N_0}}\right)^{2L}\frac{1}{(2L-1)!!}. \tag{C.9}$$

Similarly, the truncation error for $\Pr(\mathcal{B}_2)$ in (32) is bounded by

$$\begin{aligned}
&\left|\Pr(\mathcal{B}_2) - \Pr(\mathcal{B}_2;2L)\right| \\
&= \left|\frac{1}{\pi}\int_{-\infty}^{\infty}\frac{\sin(A_ku)}{u}e^{-\frac{u^2N_0}{2}} \cdot\left(\varphi_{I^I,I^Q}(u,0) - \sum_{m=0}^{L-1}b_m(-N_0)^mu^{2m}\right)du\right| \\
&< \frac{A_k}{\pi}\frac{1}{(2L)!}\left(C\sum_{k=1}^{K}\sqrt{6P_kT}\right)^{2L}\int_{-\infty}^{\infty}u^{2L}e^{-\frac{u^2N_0}{2}}du \\
&= \frac{A_k}{\pi(2L)!}\left(C\sum_{i=1,i\neq k}^{K}\sqrt{6P_iT}\right)^{2L}\int_0^{\infty}z^{L-\frac{1}{2}}e^{-\frac{zN_0}{2}}dz \\
&= \frac{A_k}{\pi(2L)!}\left(C\sum_{i=1,i\neq k}^{K}\sqrt{6P_iT}\right)^{2L}\left(\frac{2}{N_0}\right)^{L+\frac{1}{2}}\frac{(2L-1)!!}{2^L}\sqrt{\pi} \\
&= \sqrt{\frac{2A_k^2}{\pi N_0}}\left(C\sum_{i=1,i\neq k}^{K}\sqrt{\frac{6P_iT}{N_0}}\right)^{2L}\frac{1}{(2L)!!},
\end{aligned} \tag{C.10}$$

which follows from $|\sin(ax)/x| \leq |a|$ and (C.7). We also substitute u^2 with z and use [39, 3.381(4)] in (C.10).

From (26), the truncation error on the SER is bounded by

$$\begin{aligned}&\left|\mathrm{SER}_{k,m}^{\mathrm{exact}}-\mathrm{SER}_{k,m}^{(2L)}\right|\\&\quad\le\frac{(\sqrt{M_{k,m}}-1)^2}{M_{k,m}}\left|\Pr(\mathcal{B}_1)-\Pr(\mathcal{B}_1;2L)\right|\\&\qquad+\frac{2(\sqrt{M_{k,m}}-1)}{M_{k,m}}\left|\Pr(\mathcal{B}_2)-\Pr(\mathcal{B}_2;2L)\right|\\&\quad\le\frac{M_{k,m}-1}{M_{k,m}}\left|\Pr(\mathcal{B}_1)-\Pr(\mathcal{B}_1;2L)\right|\\&\qquad+\frac{2(\sqrt{M_{k,m}}-1)}{M_{k,m}}\left|\Pr(\mathcal{B}_2)-\Pr(\mathcal{B}_2;2L)\right|,\quad\text{(C.11)}\end{aligned}$$

where the last inequality is due to $(\sqrt{M_{k,m}}-1)^2\le M_{k,m}-1$ for positive $M_{k,m}$. Substituting (C.9), (C.10) and (13) into (C.11), we obtain

$$\begin{aligned}\left|\mathrm{SER}_{k,m}^{\mathrm{exact}}-\mathrm{SER}_{k,m}^{(2L)}\right|<\frac{1}{M_{k,m}}\sqrt{\frac{6P_kT}{\pi N_0}}\left(C\sum_{i=1,i\neq k}^{K}\sqrt{\frac{6P_iT}{N_0}}\right)^{2L}\\\cdot\left[\sqrt{\frac{6P_kT}{\pi N_0}}\frac{1}{(2L-1)!!}+\frac{2}{(2L)!!}\right].\quad\text{(C.12)}\end{aligned}$$

REFERENCES

[1] K. Doppler, M. Rinne, C. Wijting, C. B. Ribeiro, and K. Hugl, "Device-to-device communication as an underlay to LTE-advanced networks," *IEEE Commun. Mag.*, vol. 47, no. 12, pp. 42–49, Dec. 2009.

[2] J. A. C. Bingham, "Multicarrier modulation for data transmission: An idea whose time has come," *IEEE Commun. Mag.*, vol. 28, no. 5, pp. 5–14, May 1990.

[3] G. Wunder *et al.*, "5GNOW: Non-orthogonal, asynchronous waveforms for future mobile applications," *IEEE Commun. Mag.*, vol. 52, no. 2, pp. 97–105, Feb. 2014.

[4] J. V. D. Beek and F. Berggren, "Out-of-band power suppression in OFDM," *IEEE Commun. Lett.*, vol. 12, no. 9, pp. 609–611, Sep. 2008.

[5] G. Cherubini, E. Eleftheriou, and S. Ölcer, "Filtered multitone modulation for very high-speed digital subscriber lines," *IEEE J. Sel. Areas Commun.*, vol. 20, no. 5, pp. 1016–1028, Jun. 2002.

[6] L. Wei, R. Q. Hu, Y. Qian, and G. Wu, "Enable device-to-device communications underlaying cellular networks: Challenges and research aspects," *IEEE Commun. Mag.*, vol. 52, no. 6, pp. 90–96, Jun. 2014.

[7] O. Shimbo and M. Celebiler, "The probability of error due to intersymbol interference and Gaussian noise in digital communication systems," *IEEE Trans. Commun. Technol.*, vol. 19, no. 2, pp. 113–119, Apr. 1971.

[8] M. Celebiler and G. Coupe, "Effects of thermal noise, filtering and cochannel interference on the probability of error in binary coherent PSK systems," *IEEE Trans. Commun.*, vol. 26, no. 2, pp. 257–267, Feb. 1978.

[9] N. C. Beaulieu and J. Cheng, "Precise error-rate analysis of bandwidth-efficient BPSK in Nakagami fading and cochannel interference," *IEEE Trans. Commun.*, vol. 52, no. 1, pp. 149–158, Jan. 2004.

[10] N. C. Beaulieu and A. A. Abu-Dayya, "Bandwidth efficient QPSK in cochannel interference and fading," *IEEE Trans. Commun.*, vol. 43, no. 9, pp. 2464–2474, Sep. 1995.

[11] J. Cheng, N. C. Beaulieu, and X. Zhang, "Precise BER analysis of dual-channel reception of QPSK in Nakagami fading and cochannel interference," *IEEE Commun. Lett.*, vol. 9, no. 4, pp. 316–318, Apr. 2005.

[12] *Digital Video Broadcasting (DVB); Frame Structure Channel Coding and Modulation for a Second Generation Digital Transmission System for Cable Systems (DVB-C2)*, ETSI Standard EN 302 769, Rev. 1.3.1, Oct. 2015.

[13] K. Cho and D. Yoon, "On the general BER expression of one- and two-dimensional amplitude modulations," *IEEE Trans. Commun.*, vol. 50, no. 7, pp. 1074–1080, Jul. 2002.

[14] J. I. Montojo and L. B. Milstein, "Error rate for PSK and QAM modulations for non-ideal OFDM systems with noisy channel estimates and receive diversity," *IEEE Trans. Commun.*, vol. 59, no. 10, pp. 2703–2715, Oct. 2011.

[15] A. Javed and R. Tetarenko, "Error probability upper bound for coherently detected QASK signals with cochannel interference," *IEEE Trans. Commun.*, vol. 27, no. 12, pp. 1782–1785, Dec. 1979.

[16] C. Rivera and J. A. Ritcey, "Error probabilities for QAM systems on partially coherent channels with intersymbol interference and crosstalk," *IEEE Trans. Commun.*, vol. 46, no. 6, pp. 775–783, Jun. 1998.

[17] X. Liu and L. Hanzo, "Exact BER of rectangular-constellation quadrature amplitude modulation subjected to asynchronous co-channel interference and Nakagami-m fading," in *Proc. IEEE Wireless Commun. Netw. Conf. (WCNC)*, Mar. 2007, pp. 2216–2220.

[18] W. Zhao and S. Wang, "Resource sharing scheme for device-to-device communication underlaying cellular networks," *IEEE Trans. Commun.*, vol. 63, no. 12, pp. 4838–4848, Dec. 2015.

[19] C.-H. Yu, K. Doppler, C. B. Ribeiro, and O. Tirkkonen, "Resource sharing optimization for device-to-device communication underlaying cellular networks," *IEEE Trans. Wireless Commun.*, vol. 10, no. 8, pp. 2752–2763, Aug. 2011.

[20] G. Yu, L. Xu, D. Feng, R. Yin, G. Y. Li, and Y. Jiang, "Joint mode selection and resource allocation for device-to-device communications," *IEEE Trans. Commun.*, vol. 62, no. 11, pp. 3814–3824, Nov. 2014.

[21] R. Wang, J. Zhang, S. H. Song, and K. B. Letaief, "QoS-aware channel assignment for weighted sum-rate maximization in D2D communications," in *Proc. IEEE Global Commun. Conf. (GLOBECOM)*, Dec. 2015, pp. 1–6.

[22] W. Yu and R. Lui, "Dual methods for nonconvex spectrum optimization of multicarrier systems," *IEEE Trans. Commun.*, vol. 54, no. 7, pp. 1310–1322, Jul. 2006.

[23] Z.-Q. Luo and S. Zhang, "Dynamic spectrum management: Complexity and duality," *IEEE J. Sel. Topics Signal Process.*, vol. 2, no. 1, pp. 57–73, Feb. 2008.

[24] T. Schierl, T. Stockhammer, and T. Wiegand, "Mobile video transmission using scalable video coding," *IEEE Trans. Circuits Syst. Video Technol.*, vol. 17, no. 9, pp. 1204–1217, Sep. 2007.

[25] M. V. D. Schaar, S. Krishnamachari, S. Choi, and X. Xu, "Adaptive cross-layer protection strategies for robust scalable video transmission over 802.11 WLANs," *IEEE J. Sel. Areas Commun.*, vol. 21, no. 10, pp. 1752–1763, Dec. 2003.

[26] D. Wang, L. Toni, P. C. Cosman, and L. B. Milstein, "Uplink resource management for multiuser OFDM video transmission systems: Analysis and algorithm design," *IEEE Trans. Commun.*, vol. 61, no. 5, pp. 2060–2073, May 2013.

[27] D. Wu, J. Wang, R. Q. Hu, Y. Cai, and L. Zhou, "Energy-efficient resource sharing for mobile device-to-device multimedia communications," *IEEE Trans. Veh. Technol.*, vol. 63, no. 5, pp. 2093–2103, Jun. 2014.

[28] Q. Wang, W. Wang, S. Jin, H. Zhu, and N. T. Zhang, "Quality-optimized joint source selection and power control for wireless multimedia D2D communication using Stackelberg game," *IEEE Trans. Veh. Technol.*, vol. 64, no. 8, pp. 3755–3769, Aug. 2015.

[29] G. Fodor *et al.*, "Design aspects of network assisted device-to-device communications," *IEEE Commun. Mag.*, vol. 50, no. 3, pp. 170–177, Mar. 2012.

[30] N. C. Beaulieu and M. O. Damen, "Parametric construction of Nyquist-I pulses," *IEEE Trans. Commun.*, vol. 52, no. 12, pp. 2134–2142, Dec. 2004.

[31] N. Michailow *et al.*, "Generalized frequency division multiplexing for 5th generation cellular networks," *IEEE Trans. Commun.*, vol. 62, no. 9, pp. 3045–3061, Sep. 2014.

[32] J. G. Proakis and M. Salehi, *Digital Communications*, 5th ed. New York, NY, USA: McGraw-Hill, 2007.

[33] X.-G. Xia, "A family of pulse-shaping filters with ISI-free matched and unmatched filter properties," *IEEE Trans. Commun.*, vol. 45, no. 10, pp. 1157–1158, Oct. 1997.

[34] H. Schwarz, D. Marpe, and T. Wiegand, "Overview of the scalable video coding extension of the H.264/AVC standard," *IEEE Trans. Circuits Syst. Video Technol.*, vol. 17, no. 9, pp. 1103–1120, Sep. 2007.

[35] K. Stuhlmüller, N. Färber, M. Link, and B. Girod, "Analysis of video transmission over lossy channels," *IEEE J. Sel. Areas Commun.*, vol. 18, no. 6, pp. 1012–1032, Jun. 2000.

[36] A. Papoulis, *The Fourier Integral and its Applications*. New York, NY, USA: McGraw-Hill, 1962.

[37] N. C. Beaulieu, "A useful integral for wireless communication theory and its application to rectangular signaling constellation error rates," *IEEE Trans. Commun.*, vol. 54, no. 5, pp. 802–805, May 2006.

[38] H. Cramér, *Mathematical Methods of Statistics*. Princeton, NJ, USA: Princeton Univ. Press, 1999.

[39] I. Gradshteyn and I. Ryzhik, *Table of Integrals, Series, and Products*. San Diego, CA, USA: Academic, 2007.
[40] C. Xu, L. Song, and Z. Han, *Resource Management for Device-to-Device Underlay Communication*. Berlin, Germany: Springer, 2014.
[41] P. Henrici, *Applied and Computational Complex Analysis: Power Series, Integration, Conformal Mapping, Location of Zeros*, vol. 1. New York, NY, USA: Wiley 1974.
[42] S. G. Krantz, *Real Analysis and Foundations*, 2nd ed. Boca Raton, FL, USA: CRC Press, 2005.

Peizhi Wu (S'12) received the B.E. degree in electronic engineering from Tsinghua University, Beijing, China, in 2011, and the M.S. and Ph.D. degrees in electrical engineering from the University of California at San Diego, La Jolla, CA, USA, in 2014 and 2016, respectively.

He was with the Wireless Connectivity Group, Broadcom Inc., San Diego, CA, in 2013, and Nokia Research Center, Berkeley, CA, in 2014. He is currently a Senior System Engineer with Qualcomm Inc., San Diego, CA. His research interests are in wireless communications, video transmission, cross-layer design, and interference management.

Pamela C. Cosman (S'88–M'93–SM'00–F'08) received the B.S. degree (Hons.) in electrical engineering from the California Institute of Technology, Pasadena, CA, USA, in 1987, and the Ph.D. degree in electrical engineering from Stanford University, Stanford, CA, in 1993. From 1993 to 1995, she was an NSF Post-Doctoral Fellow with Stanford University and a Visiting Professor with the University of Minnesota. In 1995, she joined the faculty of the Department of Electrical and Computer Engineering, University of California at San Diego, La Jolla, CA. She was the Director of the Center for Wireless Communications, University of California at San Diego, from 2006 to 2008. She is currently a Professor and the Associate Dean for the Students of the Jacobs School of Engineering. Her research interests are in the areas of image and video compression and processing and wireless communications.

Dr. Cosman has been a member of the Technical Program Committee or the Organizing Committee for numerous conferences, including the ICIP 2008-2011, the QOMEX 2010-2012, the ICME 2011-2013, the VCIP 2010, the PacketVideo 2007-2013, the WPMC 2006, the ICISP 2003, the ACIVS 2002-2012, and the ICC 2012. She was an Associate Editor of the IEEE COMMUNICATIONS LETTERS (1998-2001), a Guest Editor of the 2000 Special Issue of the IEEE JOURNAL ON SELECTED AREAS IN COMMUNICATIONS on Error-Resilient Image and Video Coding, an Associate Editor of the IEEE SIGNAL PROCESSING LETTERS (2001-2005), the Editor-in-Chief (2006-2009) and a Senior Editor (2003-2005, 2010-2013) of the IEEE JOURNAL ON SELECTED AREAS IN COMMUNICATIONS. She is a member of Tau Beta Pi and Sigma Xi. Her awards include the ECE Departmental Graduate Teaching Award, a CAREER Award from the National Science Foundation, the Powell Faculty Fellowship, the GLOBECOM 2008 Best Paper Award, and the HISB 2012 Best Poster Award. She was the Technical Program Chair of the 1998 Information Theory Workshop in San Diego.

Laurence B. Milstein (S'66–M'68–SM'77–F'85) received the B.E.E. degree from The City College of New York, NY, USA, in 1964, and the M.S. and Ph.D. degrees in electrical engineering from the Polytechnic Institute of Brooklyn, Brooklyn, NY, USA, in 1966 and 1968, respectively. From 1968 to 1974, he was with the Space and Communications Group, Hughes Aircraft Company. From 1974 to 1976, he was a member of the Department of Electrical and Systems Engineering, Rensselaer Polytechnic Institute, Troy, NY. He was the Department Chair with the University of California at San Diego, La Jolla, CA, USA. Since 1976, he has been with the University of California at San Diego, where he is currently the Ericsson Professor of Wireless Communications Access Techniques, and is involved in the area of digital communication theory with special emphasis on spread-spectrum communication systems. He has been also a consultant to both government and industry in the areas of radar and communications.

Dr. Milstein was the Vice President of the Technical Affairs of the IEEE Communications Society in 1990 and 1991. He has been an Associate Editor for communication theory of the IEEE TRANSACTIONS ON COMMUNICATIONS, an Associate Editor of book reviews of the IEEE TRANSACTIONS ON INFORMATION THEORY, an Associate Technical Editor of the IEEE *Communications Magazine*, and the Editor-in-Chief of the IEEE JOURNAL ON SELECTED AREAS IN COMMUNICATIONS. He was a recipient of the 1998 Military Communications Conference Long Term Technical Achievement Award, the Academic Senate 1999 UCSD Distinguished Teaching Award, the IEEE Third Millennium Medal in 2000, the 2000 IEEE Communications Society Armstrong Technical Achievement Award, and various prize paper awards, including the 2002 Fred Ellersick MILCOM Award. He was also a recipient of the IEEE Communication Theory Technical Committee (CTTC) Service Award in 2009 and the CTTC Achievement Award in 2012. He was the Chair of the IEEE Fellows Selection Committee.